MICROCOPY RESOLUTION TEST CHART

NATIONAL BUREAU OF STANDARDS-1963-A

AFWAL-TR-82-2113

ADA129681

NUMERICAL MODELLING OF RAMJET COMBUSTORS

Warren H. Harch

Ramjet Technology Branch
Ramjet Engine Division
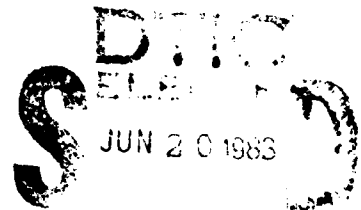
February 1983

Final Report for Period October 1981 - August 1982

Approved for public release; distribution unlimited.

AERO PROPULSION LABORATORY
AIR FORCE WRIGHT AERONAUTICAL LABORATORIES
AIR FORCE SYSTEMS COMMAND
WRIGHT-PATTERSON AIR FORCE BASE, OHIO 45433
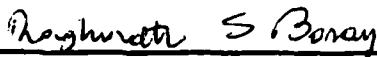
DTIC
ELECTE
JUN 2 0 1983

83   06   20   009

NOTICE

When Government drawings, specifications, or other data are used for any purpose other than in connection with a definitely related Government procurement operation, the United States Government thereby incurs no responsibility nor any obligation whatsoever; and the fact that the government may have formulated, furnished, or in any way supplied the said drawings, specifications, or other data, is not to be regarded by implication or otherwise as in any manner licensing the holder or any other person or corporation, or conveying any rights or permission to manufacture, use, or sell any patented invention that may in any way be related thereto.

This technical report has been reviewed and is approved for publication.

RAGHUNATH S. BORAY
Project Engineer
Ramjet Technology Branch
Ramjet Engine Division
Aero Propulsion Laboratory

FRANK D. STULL, Chief
Ramjet Technology Branch
Ramjet Engine Division
Aero Propulsion Laboratory

FOR THE COMMANDER:

WILLIAM G. BEECROFT
Deputy Director
Ramjet Engine Division
Aero Propulsion Laboratory

REPORT DOCUMENTATION PAGE		READ INSTRUCTIONS BEFORE COMPLETING FORM
1. REPORT NUMBER AFWAL-TR-82-2113	2. GOVT ACCESSION NO.	3. RECIPIENT'S CATALOG NUMBER
4. TITLE (and Subtitle) NUMERICAL MODELLING OF RAMJET COMBUSTORS		5. TYPE OF REPORT & PERIOD COVERED Final Report Oct 1981 - Aug 1982
		6. PERFORMING ORG. REPORT NUMBER
7. AUTHOR(s) Warren H. Harch		8. CONTRACT OR GRANT NUMBER(s)
9. PERFORMING ORGANIZATION NAME AND ADDRESS Ramjet Technology Branch Ramjet Engine Division		10. PROGRAM ELEMENT, PROJECT, TASK AREA & WORK UNIT NUMBERS 2308S101
11. CONTROLLING OFFICE NAME AND ADDRESS Aero Propulsion Laboratory (AFWAL/PORT) Air Force Wright Aeronautical Laboratories, AFSC Wright-Patterson AFB, OH 45433		12. REPORT DATE February 1983
		13. NUMBER OF PAGES 65
14. MONITORING AGENCY NAME & ADDRESS(if different from Controlling Office)		15. SECURITY CLASS. (of this report) Unclassified
		15a. DECLASSIFICATION/DOWNGRADING SCHEDULE
16. DISTRIBUTION STATEMENT (of this Report) Approved for public release; distribution unlimited.		
17. DISTRIBUTION STATEMENT (of the abstract entered in Block 20, if different from Report)		
18. SUPPLEMENTARY NOTES Author was a visiting scientist at AFWAL/PORT, on leave from Aeronautical Research Laboratories, Australia under the support of an Australian Public Service Board Scholarship.		
19. KEY WORDS (Continue on reverse side if necessary and identify by block number) computer modelling ramjets combustors		
20. ABSTRACT (Continue on reverse side if necessary and identify by block number) The present work deals with the development of computer codes for modelling of gas turbine combustors to ramjet combustor configurations. In particular, the STARPIC code of Lilley and Rhode has been expanded to include reacting compressible flows.		

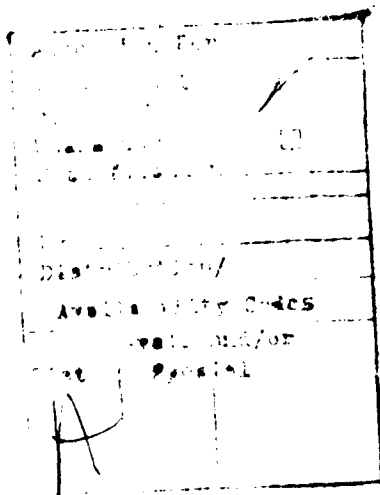DD FORM 1 JAN 73 **1473** EDITION OF 1 NOV 68 IS OBSOLETE

TABLE OF CONTENTS

LIST OF ILLUSTRATIONS

SECTION I

INTRODUCTION

In recent years there has been a reawakening of interest in the use of ramjet propulsion systems for modern strategic and tactical missiles. The advantages of ramjet propulsion are the high specific impulse (resulting in enhanced range and/or speed capability) and a conceptually simple system requiring no moving parts other than those associated with the fuel control system. The main disadvantage has been that a booster system is required to provide the high initial velocity for the propulsion system to operate.

The modern ramjet technology employs the integral rocket ramjet concept where sequential use is made of the ramjet chamber as a solid rocket combustion chamber (for the initial boost stage of flight) followed by its later use as a ramjet combustion chamber (after the solid fuel has been burned and high velocity attained). Two conceptions for the integral rocket/ramjet configuration are shown in Figures 1a, b, and c.

One of the more critical problem areas in the integral rocket/ramjet is the ramjet combustion cycle. Since the ramjet combustor must serve the dual purpose as housing for rocket propellant, it cannot be ideally configured in terms of fuel injection, flameholders, and combustor geometry for operation in the ramjet mode. One basic combustor design is shown in Figure 1b. In this type of combustor, fuel injection takes place in the air inlet duct upstream of the dump station. Flow recirculation in the region just downstream of the dump station serves as the primary flameholding mechanism. This may be supplemented by swirling of the inlet air.

A second combustor design is shown in Figure 1d. In this configuration, hot fuel rich gas from a solid fuel gas generator enters the dump from a small jet and mixes with air from multiple circumferentially located air inlets. Again, flow recirculation provides flame stabilization.

1
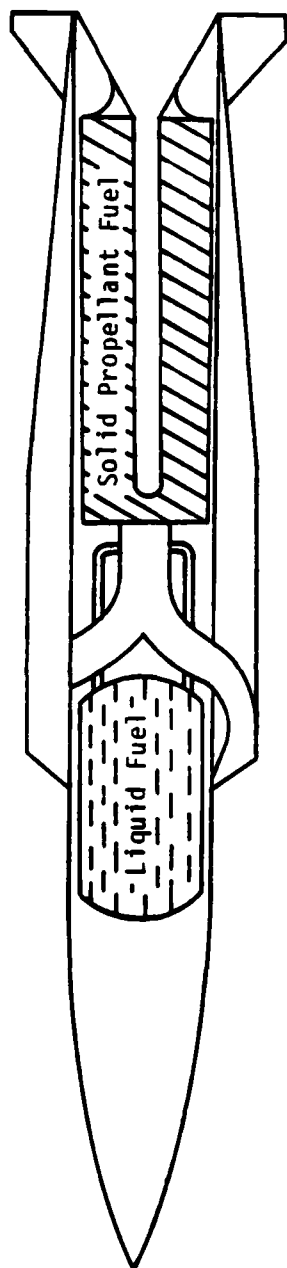
Figure 1a. Integral Rocket/Ramjet Missile
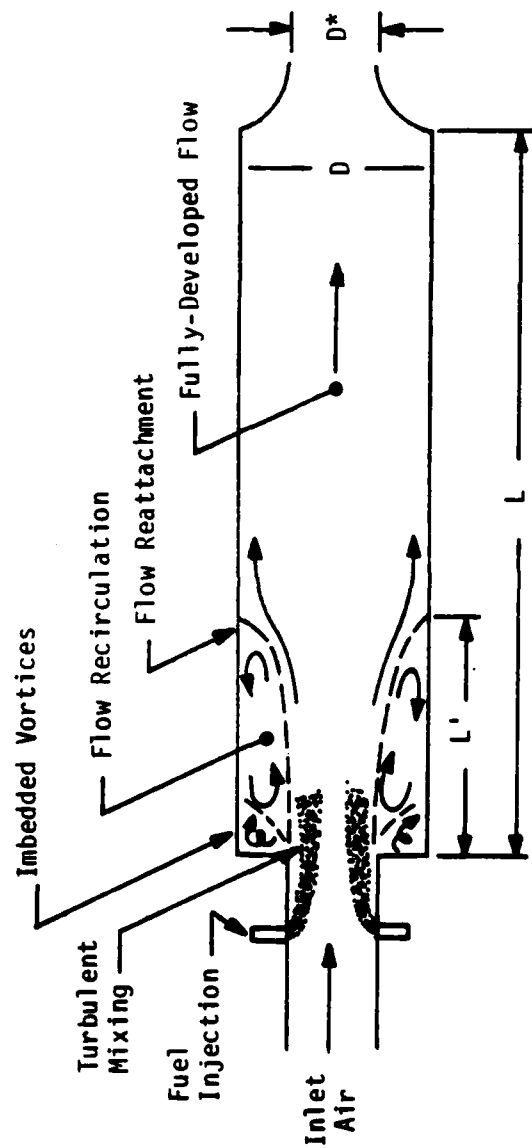
Figure 1b. Ramjet Combustor Flowfield
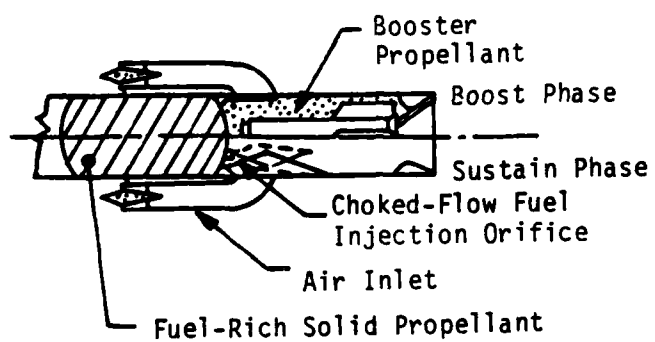
Figure 1c. Ducted Rocket Components
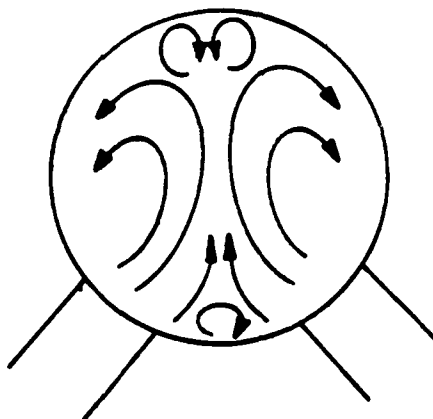
Figure 1d. Typical Flow Cross Section for Side Inlet Combustor

As indicated in these simple sketches, the combustion flow is multiphase, turbulent, and involves flow separation and large recirculation regions. In addition, many ramjet combustors of interest contain fully 3-D flowfields because of multiple air inlets located at discrete circumferential locations as illustrated in Figures 1c and d.

The present work is concerned with the computer modelling of the ramjet combustor flowfields and is part of several concurrent theoretical and experimental efforts undertaken to gain further insights into the characteristics of these type of flowfields.

SECTION II

PREVIOUS WORK

The modelling of ramjet combustors has been recently summarized by Lilley (Reference 1). In his paper, Lilley outlines two approaches which can be distinguished as simplified models and Navier-Stokes type solvers. The simplified models of the flow in the past have been very popular (Refrences 2 through 6) since they avoid the problem of solving partial differential equations by dividing the flow into regions such as perfectly stirred reactors, well stirred reactors and plug flow reactors with separate simple empirical models for each region. These models may give useful qualitative trends.

In recent years, however, there has been a dramatic increase in the popularity of methods based on the direct numerical solution of the Navier-Stokes equations for combusting flow. Increases in the understanding of physical phenomena, computing power, numerical algorithm efficiency, and cost of experiments have all contributed to this trend. The trend has been the greatest in the area of gas turbine and furnace design and today major engine manufacturers use numerical codes in their combustor design process to predict performance trends, predict durability problem areas, and reduce testing. Since the codes need to calculate the value of all dependent variables in the governing equations for all points in the flow, the distribution of a property such as density (for which no suitable experimental measurement method presently exists) can be determined by these models. Modification of these codes for the application to ramjet combustor design is a feasible proposition (References 7, 8). The aim of this report will be to outline present work at AFWAL/PORT involving adapting and modifying developed numerical codes to the ramjet geometry and flow conditions. Areas in which future research is needed will also be outlined.

SECTION III

THEORETICAL BACKGROUND

The basis of any numerical model of combusting flow is a set of partial differential equations that govern the flowfield and chemistry of the particular regime of interest. Formulation of these equations necessitates modelling of physical phenomena. The general structure of a numerical code is outlined in Figure 2.

There is wide variation between codes regarding solution technique (Reference 9) and the sophistication and extent to which various physical effects are included. The codes at AFWAL/PORT include a simple code for modelling 2-D isothermal recirculating flow and a relatively complex code for modelling a three-dimensional multiphase combustor.

The codes in this report all proceed in the following manner. The ensemble averaged Navier-Stokes equations for the steady turbulent flow of a viscous fluid in which turbulent density fluctuations are ignored and the transport equations for an ensemble averaged scalar variable may all be written in the following similar form (cylindrical polar coordinates).

$$\frac{1}{r} \left[\frac{\partial}{\partial x} (\rho r U \phi) + \frac{\partial}{\partial r} (\rho r V \phi) - \frac{\partial}{\partial x} (r \Gamma_\phi \frac{\partial \phi}{\partial x}) - \frac{\partial}{\partial r} (r \Gamma_\phi \frac{\partial \phi}{\partial r}) \right] = S_\phi \qquad (1)$$

The term ϕ is a general dependent variable and the equation isolates the terms for the convection of ϕ, diffusion (via turbulent flux terms of ϕ) and the source (both creation and dissipation) of ϕ. The equations differ not only in their exchange coefficient Γ_ϕ but also, and primarily, in their source term, S_ϕ. Terms such as pressure gradients and chemical reactions are treated in the generalized source S_ϕ.

To provide closure of the equations, it is necessary to model the turbulence. The method used in this work is the familiar k-ϵ (Reference 10)

6
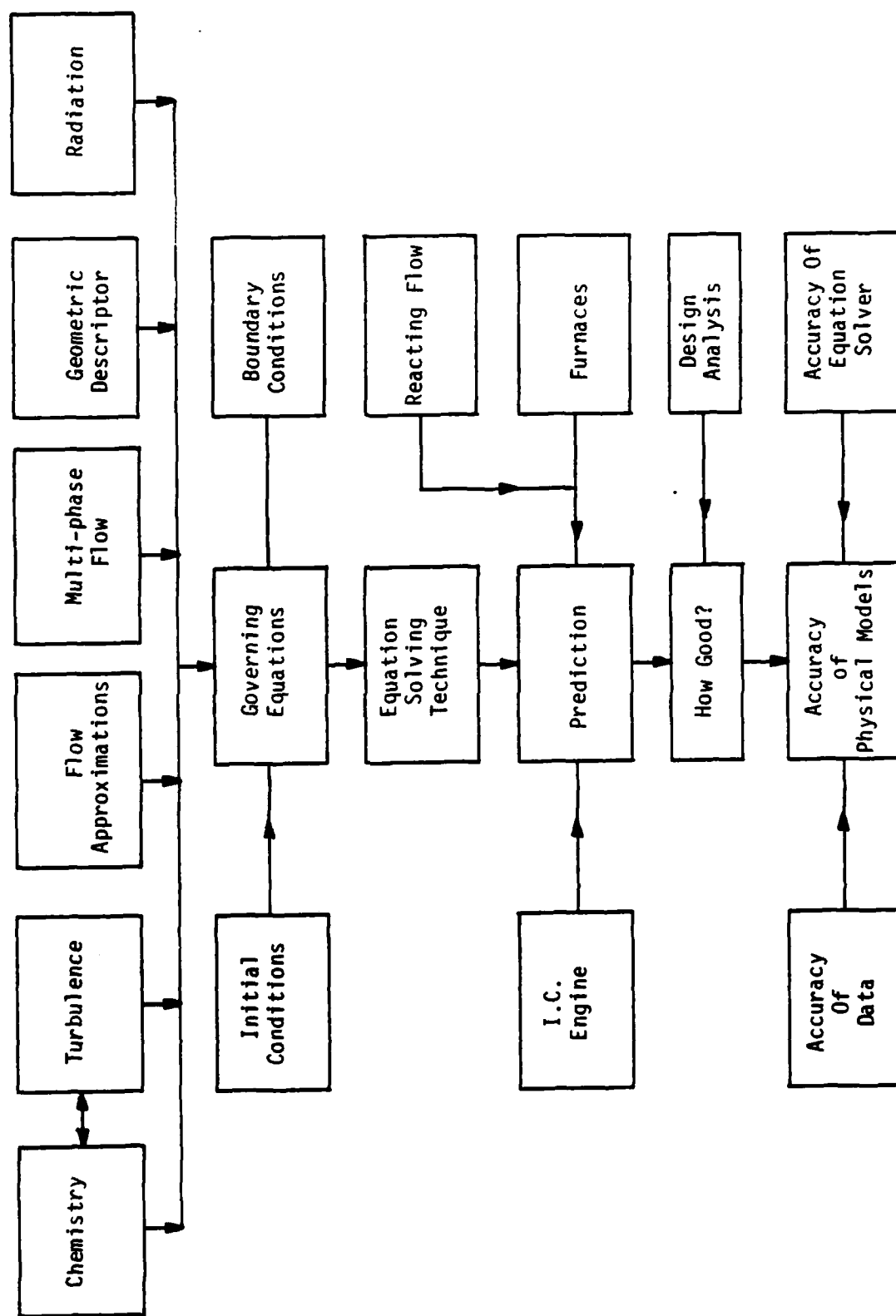
Figure 2. Numerical Code Structure

model in which the eddy viscosity μ can be defined in terms of the scalar quantities, turbulence energy k and turbulence dissipation rate ϵ as in Equation 2.

$$\mu = C_\mu \frac{\rho k^2}{\epsilon} \qquad (2)$$

For a description of a 2-D axisymmetric isothermal flow, the equations may be solved for ϕ equal to the axial, radial, and swirling velocities (u,v,w), the turbulent kinetic energy k and turbulent dissipation rate ϵ with the exchange coefficients and source terms outlined in Table B-1. Note, however, that the equations could also be solved for fuel fraction. mixture fraction, stagnation enthalpy, and possibly other variables as well. Note also that no transport equation exists for pressure and that the velocity terms must also satisfy the continuity equation. The solution to this dilemma is to determine the pressure from the Poisson equation (a combination of the continuity and momentum equations).

The technique used for the solution of the differential equations is based on the TEACH program (References 11, 12). A finite difference primitive variable (velocities and pressure) procedure is used. An initial guess is made for pressure and the equations solved for velocity terms on ASD CDC computer. Corrections are then made to velocity and pressure to ensure continuity and the remaining equations are solved. An implicit line-by-line relaxation technique is used in the solution procedure. A staggered grid system is used in which the vectors are located midway between the points at which scalars are calculated (Figure 3). Walls are simulated by the staircase method in which the boundaries are drawn between the points at which the scalars are calculated.

The finite difference equations for each ϕ are obtained by integrating equation 1 over the appropriate control volume and expressing the result in terms of neighboring grid point values. The convection and diffusion
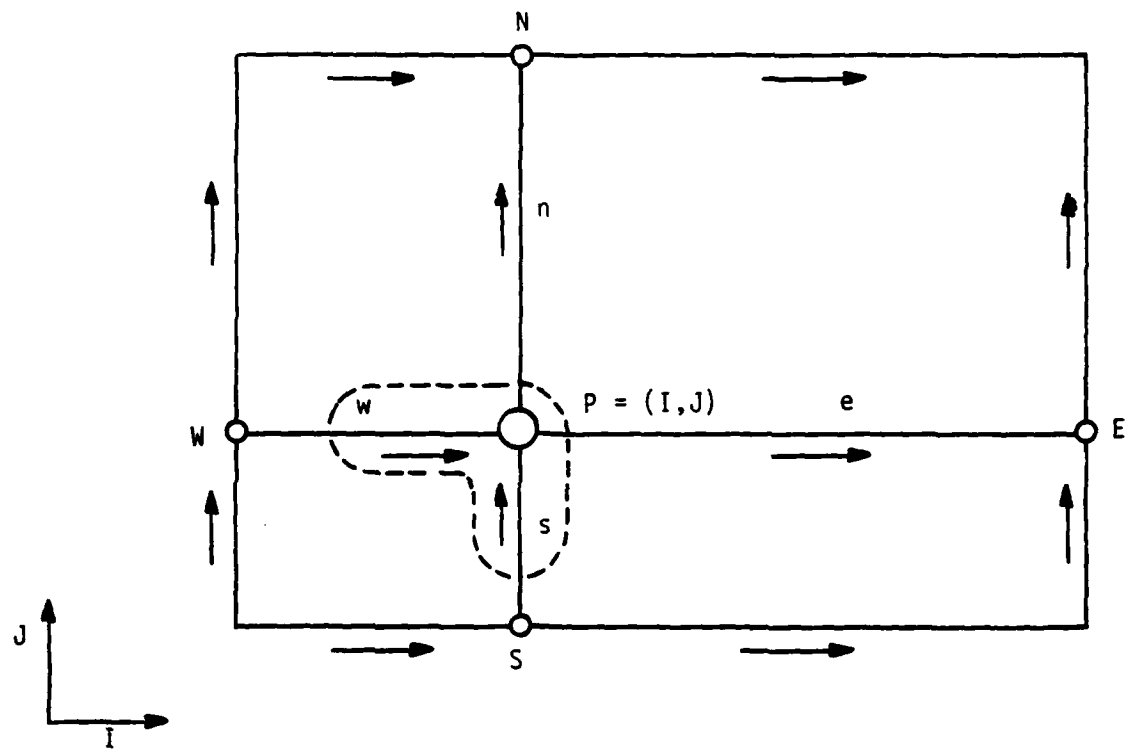
THREE GRIDS: FOR p, w ETC. - AT POSITION MARKED (O)
               FOR u VELOCITY- AT POSITION MARKED (→)
               FOR v VELOCITY- AT POSITION MARKED (↑)

Figure 3. Staggered Grid and Notation for the Rectangular
           Computational Mesh

9

terms are expressed as surface integrals and the source term is summarized resulting in an equation of the form.

$$[\rho U\phi - \Gamma_\phi \frac{\partial \phi}{\partial x}]_e A_e - [\rho U\phi - \Gamma_\phi \frac{\partial \phi}{\partial x}]_w A_w + [\rho V\phi - \Gamma_\phi \frac{\partial \phi}{\partial r}]_n A_n - [\rho V\phi - \Gamma_\phi \frac{\partial \phi}{\partial r}]_s A_s =$$

$$[S_p^\phi \phi + S_u^\phi] \times Vol \tag{3}$$

To enhance convergence, only terms which are negative are permitted in S_p^ϕ.

Boundary conditions are problem dependent; however, the following general conditions apply. Inlet values are directly specified. At the outlet, axial velocities are calculated to ensure mass continuity, radial velocities are set to zero and zero normal gradient is specified for remaining terms. Near wall tangential velocities are connected to their zero wall values by way of tangential shear stress wall functions. Near wall values for ε are fixed using length scales near the wall and the current value of k.

SECTION IV

PRESENT CODES AT AFWAL/PORT

There are at present five numerical codes at AFWAL/PORT and these are briefly outlined below.

1. TEACH-X

This is a basic version of the Imperial College Teach Code suitable for isothermal, 2-dimensional recirculating turbulent flows. The code solves u and v velocity components, pressure, turbulence kinetic energy and turbulence dissipation in isothermal, incompressible flow. The program input is designed for dump combustors.

2. TEACH-T

This code is similar to TEACH-X but includes two extra equations; one for the transport of a second species, and one for the transport of specific enthalpy. The mixture fraction and temperature (determined from the enthalpy) in conjunction with the equation of state determine the density fluctuations in the flowfield. Note that the fluid kinetic energy terms have been neglected in the enthalpy equation. The program includes combustion only to the extent that a single product is produced by instantaneous ignition and infinitely rapid reaction kinetics. This first approximation is only suitable for diffusion limited combustion where there is no initial mixing of fuel and air. The program inputs are designed for a dump type combustor equipped with a concentric annulus burner at the dump plane.

3. STARPIC

The title of this code is an acronym for swirling turbulent axisymmetric recirculating flows in practical isothermal geometries. The code was prepared by D. G. Lilley and D. L. Rhode of Oklahoma State University under NASA grant NAG-3-74 (Reference 7). This code is similar to the Teach-X code previously described except that an equation

11

for a swirl velocity component is included. The code was written
essentially to model the flow in turbine combustors and the subroutine
that specifies the initial conditions is somewhat more flexible than the
TEACH codes. The inlet conditions may include a sloping upstream
boundary which is modelled within the calculation regime by a series of
boundary steps.

Provision is also made to read the initial conditions from a previous
solution tape. This procedure is handy but does not fulfill the role of
a true restart capability since it is necessary to run the solution to
completion to obtain the solution tape; and if the job is aborted through
some calculation error or job time limit, the solution derived by the
program at that stage is lost.

The program also includes routines for calculation of non-dimensional
values, stream functions, and plot files. These are useful calculations
but would be better included in a post processor since they are
extremely wasteful of memory space.

The program contains variable underelaxation. At present, this is
in a somewhat primitive form in that the underelaxation factors increase
linearly between fixed values according to some preset conditions
determined by the programmer. Winterfeldt has indicated that considerably
improved convergence can be achieved by relating the underelaxation
factor to actual values of the local variables and geometry (Reference 13).
This is in accordance with the general experience of high underelaxation
factors leading to divergence of the solution and low underelaxation factors
leading to excessively long convergence times. Nevertheless, it should
be stated that the use of even the present method of varying the underelax-
ation factor which places considerable reliance on the experience of the
programmer is superior to the retention of fixed underelaxation factors.

4. STARRC

This title is acronymmous for Swirling Turbulent Axisymmetric
Recirculating and Reacting Compressible Code. This code was written by the

present author using the aforementioned STARPIC as a base code to which
several features were added. The diffusion equation from TEACH-T was
added together with the enthalpy equation except that the enthalpy could
now be either the specific static or stagnation enthalpy as determined
by a logic switch. The inclusion of the equation of state for calculation
of density together with the stagnation enthalpy equation allows
isentropic compressibility effects to be included. Note, however, the
solution of the pressure equation has not yet been altered to include
variations in density so that the solution tends to be explicit rather
than implicit with resultant convergence problems. The boundary conditions
allow the inclusion of a sloping upstream boundary and a downstream exit
nozzle both of which are modelled by a series of finite steps. An
expanding or an expanding-contracting grid can automatically be generated
in the x direction. The first approximation combustion of the TEACH-T
code has been included and provision made for the planned addition of
reaction kinetics. A post processor for producing various 2-dimensional
and 3-dimensional plots has been written by Schwartzkopf for this code.
The format for inputting initial conditions is somewhat more general
than that of the STARPIC code on ASD CDC computer.

The entire code has been written as a series of correction decks for
Lilley's STARPIC Code on ASD CDC computer.

5. THE 3-D CODE PERFORMANCE MODEL PROGRAM

This program was prepared for NASA under contract NAS3-22542 by
Garrett Turbine Engine Company (Reference 14) and is the extension of an
earlier code produced for the US Army and described in Report No USARTL-
TR-55C. The 3-D program is general and capable of predicting recirculating
flows in 3-dimensional geometries. At present, the code inputs and
boundary conditions are specifically oriented towards gas turbine
combustor geometries. Reacting or non-reacting, swirling or non-swirling,
diffusion and/or premixed flames, and gaseous and/or liquid fuel combustion
can be handled by the program. The code solves for all the quantities
of STARRC in a 3-dimensional flowfield plus the mass fractions of

unburned fuel, oxygen, carbon monoxide, C_xH_{y2} (the intermediate Hydrocarbon in a four step reaction) H_2, CO_2 and H_2O, three radiation flux vectors, soot and NO_x emissions and the fuel spray trajectory, droplet size distribution, and evaporation rate.

The program includes the following physical models:

a. Turbulence - the two equation (k-ϵ) turbulence model

b. Chemistry - A four step chemical reaction scheme as outlined below

$$C_xH_y \rightarrow C_xH_{y-2} + H_2$$

$$C_xH_{y-2} + \frac{x}{2} O_2 \rightarrow xCO + \frac{y-2}{2} H_2$$

$$CO + \tfrac{1}{2}O_2 \rightarrow CO_2$$

$$H_2 + \tfrac{1}{2}O_2 \rightarrow H_2O$$
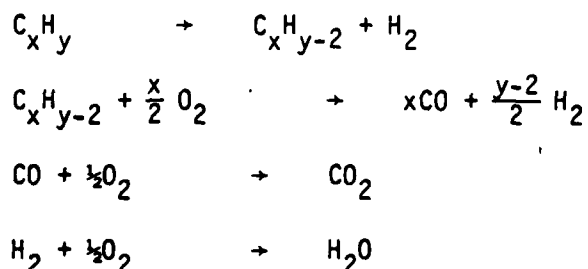
c. Chemical Reaction Rate

The reaction rates are governed by the minimum of either the time averaged Arrhenius model of the reaction kinetics or the component mixing rate as determined by a turbulent eddy break up model.

d. Soot Emissions

The program contains a quasiglobal model that requires the solution of transport equations for the concentration of nuclei and soot. Two particle sizes for soot are assumed, a small size resulting from nucleation and a large size resulting from fuel droplet pyrolosis and char formation.

e. Radiation

A six flux model is used. The absorption coefficient is calculated locally as a function of concentration of soot, carbon dioxide, and water vapor.

f.   NOx emissions

NOx emissions are calculated using the CREK kinetic model.

A typical solution procedure using the Garrett Code involves three steps executed automatically in the following manner:

(1)   Solution of all required variables except soot radiation and NOx till cumulative mass residual of approximately 5% is reached.

(2)   Inclusion of soot and radiation in the solution procedure and continue till cumulative mass residual of 1% is reached.

(3)   Inclusion of NOx equations and continue solution until the desired convergence level for the final solution (approx. 0.5%) is reached.

The present application of these five codes is directed primarily towards the use of STARRC and the NASA-Garrett 3-D Code. STARRC is suitable for axially symmetric cold flows and is configured for operation on the AFWAL CDC 7600 computer for geometries of Figure 1c. The NASA-Garrett Code is suitable for 3-dimensional geometries and is presently being configured for operation on both the AFWAL computer and the Cray computer at Kirtland AFB for geometries of Figure 1d. Both of these codes are receiving further development and will be further detailed in the following sections.

At the time of writing this report, a sixth code is being prepared to model isothermal flow in the three dimensional geometries of Figure 1d. Since this code will not contain the dependent variables associated with combustion processes, it will be far more conservative in memory requirements and consequently will allow greater resolution than the NASA-Garrett code. This code will be supplementary to the NASA-Garrett code and will principally be used for the modelling of water tunnel and cold gas flows in the geometries of Figure 1d.

SECTION V

THE COMPUTER CODE STARRC

1. INTRODUCTION

As mentioned previously, the STARRC code draws heavily on Lilley's STARPIC Code (Reference 7) and has in fact been written as a series of UPDATE correction decks to the STARPIC Code. These correction decks will be outlined and the following sections should be read in conjunction with Lilley's report.

The present program library version of STARRC incorporates all these correction sets in a resequenced format with the exception of the common block correction sets. The correction sets are discussed individually simply to outline their individual reasons for inclusion and are not separately identified in the resequenced format.

A brief description of the operation of STARRC and the STARRC post processor (intended as a supplementary users manual) and a summary of present experience follows the correction deck descriptions.

2. CORRECTION DECK DESCRIPTIONS

a. NEWCOMMON 9624, NONONDIM4824

These two correction decks modify the common blocks and the definition of IT, JT (indices of maximum dimensions of dependent variables) to allow the array structures to accommodate the required grid size. NEWCOMMON 9624 allows a 96 x 24 grid and simple editing of values 96 and 24 will allow any desired grid size. NONONDIM4824 modifies to a 48 x 24 grid and removes the nondimensional and stream function calculation routines. This enables a 48 x 24 grid problem to be run within the day shift memory restriction of $170,000_8$ words.

b. Ident DREWGRID

This correction set applies the boundary conditions for one case of the DREWRY (Reference 15) experiment discussed (Case 1).

c. Ident CALCFR

This correction deck solves the finite difference equation for the transport of mixture fractions.

d. Ident CALCH

This correction deck solves the finite difference equation for the transport of enthalpy.

e. Ident COMBUST

This correction deck modified the main controlling subroutine and property calculation subroutine to include the calculations of density, mixture fraction, and enthalpy. Density may be fixed for the case of fixed density isothermal flow or calculated from the equation of state using the local values of absolute pressure, mixture fraction and temperature. If stagnation enthalpy is calculated (INMACH = .TRUE. and INCALCH = .TRUE.), compressibility effects will be included since local temperature, and hence local density, will be determined from local enthalpy.

f. Ident COMCOM

This correction set modified the common blocks to include the enthalpy and fuel mixture fraction terms.

g. Ident COMPRO

This correction set modified the subroutine PROMOD to include chapters for enthalpy and fuel mixture fraction.

h. Ident CORECT

This set provides minor corrections to Lilley's original code

i. Ident ENERGY

This correction set alters the way in which the zero axial gradient condition is applied at the exit plane. The enthalpy values at the last axial grid points are gradually altered from initial values to ensure conservation of energy. This modification was included in an attempt to improve the convergence for nonadiabatic combustor walls in future calculations.

j. Ident INLET

This ident provides code to automatically generate a stepped grid for a sloping inlet wall. The input parameter is inlet axial length, ALINLT. The code generates steps about a curve defining the expansion of the wall radius from inlet radius to combustor radius. The general curve describing the wall radius is, at present, a linear expansion; however, other curves may easily be substituted. This ident made obsolete a previous correction deck ENTRAN which generated a dump inlet only.

k. Ident EXIT

This ident provides code to automatically generate a stepped grid for simulation of an exit nozzle. The code also supplies the boundary conditions necessary for an exit nozzle. There are two input parameters, ALTRAN and JEXIT. ALTRAN is the axial distance from the combustor inlet to the point at which the transition to the radial reduction of the nozzle occurs. JEXIT is the J index of the grid point located immediately inside the exit radius. The code generates steps about a curve describing the radius of the nozzle as a function of axial location. Two general curves have been programmed - a linear contraction and a convex elliptical contraction.

1. Idents - ROGRID, ROGFLO, RUNDAT

These correction decks provided the grid dimensions, flow data, and run data for a typical test case.

m. Ident NEWSWIRL

This ident was written to include inlet swirl in the form of a free vortex profile used in the experiments of Buckley et al (Reference 16). Note the redefinition of the parameter NSBR for defining type of swirl. A new parameter is RHUB. This determines the radius within which the inlet swirl·is considered to have solid body rotation irrespective of the nature of the remainder of the swirl profile. Note the definition of inlet solid body swirl velocity in terms of input swirl number as supplied by Lilley (Equation 4). This contrasts with the definition by Buckley (Equation 5) though the methods of the authors for calculation of swirl number for a given flow are identical

$$W = \frac{SWNB}{1*SWNB} * U * \frac{R}{Rstep} \tag{4}$$

$$W = SWNB * U * \frac{R}{Rstep} \tag{5}$$

SWNB = Input Swirl Number

n. Ident REPAIR

This ident contains miscellaneous corrections to the code. These have been written in response to problems discovered in the operation of the code. These problems may have resulted from inclusion of other correction sets or simply from the way the initial conditions were specified.

o. Ident TITLE

This ident added comment cards.

p. Ident OPGRID, CHGRID

These correction decks enable the optional selection of a grid spacing that geometrically increases in the axial direction away from the inlet plane, or alternately, a grid spacing that geometrically increases from both the inlet plane and the nozzle exit plane towards the center of the combustor.

q. Obsolete Idents may appear in the list of idents in the program library. These obsolete idents include MODIFY and XXX.

3. OPERATIONAL DETAILS OF THE STARRC CODE

The STARRC code contains 16 subroutines. The flow chart for the program is shown in Figure 4. The functions of the individual subroutines can be summarized as follows:

a. MAIN

Controls and monitors the entire sequence of calculations: initialization, properties and initial output; the iteration loop with calls to update main variables, other mixture properties and intermediate output; and, after termination of the iteration loop, final output, an increment in inlet degree of swirl and a return to the beginning again.

b. INIT

Sets values to the numerous geometric quantities concerned with grid structures, and initalizes most variables to zero or other reference value.

c. PROPS

Updates the fluid properties via sequential calculation of mass fractions of fuel oxidizer and products, temperature, density and turbulent viscosity. Uses underrelaxation for the last two of these, the k-ϵ turbulence model and appeals to PROMOD for any other modifications.

MAIN CONTROLLING
SUBROUTINE
'CONTRO'
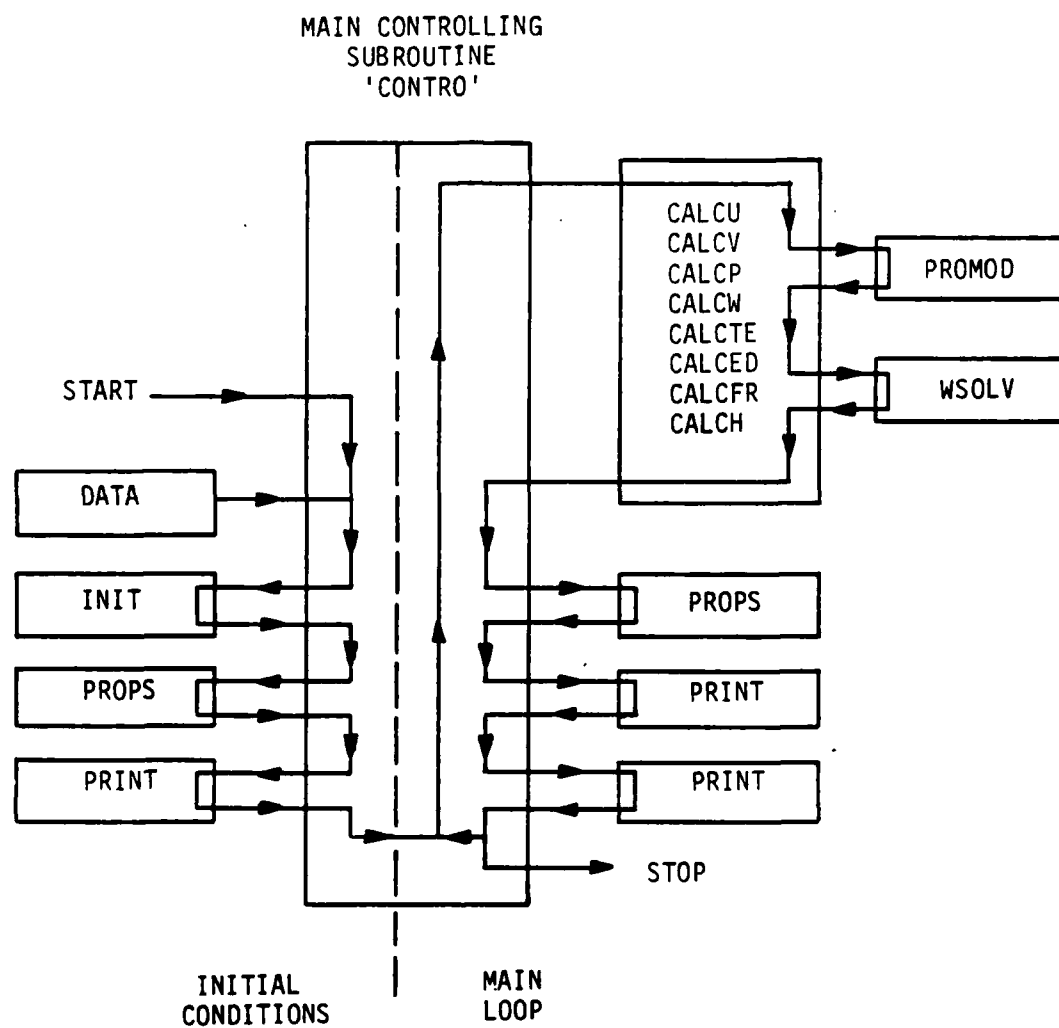
Figure 4.   STARRC Flowchart

d. PRINT

Prints out an entire variable field according to a standard format.

e. CALCU and CALCV

Calculates coupling coefficients of finite difference equation for axial velocity u* and radial velocity v*. calls PROMOD for boundary modifications and LISOLV for entire field of variables to be updated to get u* and v* fields.

f. CALCP

Calculates coupling efficients of finite difference equation for pressure correction p'; calls PROMOD for boundary modifications and LISOLV to obtain p' field. The subroutine closes with p*, u* and v* being 'corrected' with p', u', and v'.

g. CALCW, CALCTE, CALCED, CALCFR, CALCH

Calculates coupling coefficients of appropriate finite difference equation, calls appropriate part of PROMOD and then LISOLV for complete update of the variable in question.

h. PROMOD

Modifies the values of the finite difference equation coefficients, or the variables, near walls or other boundaries where particular conditions apply. The subroutine is divided into chapters, each handling a particular variable and being called from a CALC subroutine, and each chapter considers all the boundaries around the solution domain.

i. LISOLV

Updates entire field of a particular variable, by applying TDMA (tridiagonal matrix algorithm) to all the lines in the r-direction sequentially from left to right of the integration domain.

From this description it can be seen that in general the user is interested in making modifications to only 3 subroutines; CONTRO, PROPS and PROMOD with the majority of corrections being applied to subroutine CONTRO. In the present format the code does not read any input. All input data (other than restart data) is contained as Fortran statements and recompilation is necessary for each execution. The normal operating procedure is therefore to write the input code as a correction set to the basic code. This premise is used in the operating instructions set out below.

The following instructions are referenced to subroutine name and line number (STARRC, CY = 15) and are intended as an operational checklist for the novice to use in conjunction with Lilley's report (Reference 7).

1. Set Common Block Sizes and values for IT and JT using NEWCOMMONnn or NONONDIMmm.

2. CONTRO.88 CONTRO.89

Data block entries for swirl numbers and/or vane blade angles for the solution of problems with swirl. The program always assumes that swirl is present so that to solve for only the zero swirl case it is necessary to specify a single solution and set the first parameters of the swirl data block equal to zero.

3. CONTRO.96

This statement deletes error messages resulting from exponent underflow and sets the variable for which the error was detected to zero.

4. CONTRO.98 CONTRO.118

Logical switches. The majority of these are self explanatory, however the following rules may be helpful.

a. With the present parameters, IFINE = .FALSE. implies a coarse grid of 48 points in the axial direction. Of these 48 points, 45 are

23

generated to cover the specified geometry and 3 (set by NEXRAC) are set
for constant diameter geometry downstream of the exit. The axial locations
for these last 3 points are obtained by reflecting the previous 3 points
about the exit plane. If IFINE = .TRUE., a fine grid is generated with
96 points in the axial direction. Of these 96 points, 91 are located
within the specified geometry, and 5 (set by NEXRAF) are set for constant
diameter geometry downstream of the exit and their axial location is
determined by reflection of the previous 5 points about the exit plane.

b. INCONT = .TRUE. implies that the grid spacing in the axial
direction expands to the center of the combustor and then contracts at
the same rate to the exit plane of the combustor. If INCONT is set to
.FALSE., the grid spacing will continue to expand in the axial direction
to the exit plane of the combustor.

c. INMACH = .TRUE. implies calculation of stagnation enthalpy rather
than static enthalpy.

d. INREAC = .TRUE. implies chemical reaction occurs.

e. IROTEM = .FALSE. implies fixed density isothermal flow.
IROTEM = .TRUE. implies calculation of density from equation of state.
If INMACH, IROTEM and INCALH are all set .TRUE. compressibility effects
are included in the flow calculations.

5. CONTROL.122 - see instruction 52.

6. CONTROL.124 - NSTLN = n. The value n sets the number of streamlines
calculated. The default value is 11.

7. CONTRO.125 - NPLTLN = n. The value n sets the number of streamlines
plotted on the line printer plot. The default value is 6.

8. CONTRO.126 - MAXLN = n. The value n sets the maximum number of
streamlines that may be plotted. The default value is 10.

9. CONTRO.128 - JPRINT = NITER + n. The value n determines the number iterations between printing of field variable values. The default value is 1100.

10. CONTRO.129 - IPRINT = NITER + n. The value n determines the number of iterations between printing residual sums and monitor values of field variables. The default value is 1.

11. CONTRO.130 - LFS = n. The value n sets the index of the vane blade angle array or the index of the swirl number array for the first swirl calculation. The default value is 1.

12. CONTRO.131 - LFSMAX = n. The value n sets the index of the vane blade angle array or the index of the swirl number array for the last swirl calculation. The default value is 1.

13. CONTRO.133 - MAXIT = NITER + n. The value n is the maximum number of iterations to be run for each swirl case if the solution is not stopped by either a convergence or a divergence criterion. The default value is 1000.

14. CONTRO.132 - NSBR = n. The value n determines the type of swirl profile. Three values for n are presently recognized.

   a. n = 1 Solid Body Rotation from Swirl Generator

   b. n = 2 Flat Swirl Profile from Swirl Vanes

   c. n = 3 Free Vortex Swirl Profile

The present default value is 1.

15. CONTRO.135 CONTRO.136 - IT = m JT = n. See instruction 1.

16. CONTRO.138 CONTRO.145 - NSWP$\emptyset$ = $n_\emptyset$ - The value $n_\emptyset$ sets the number of application of the line iteration for the solution of the $\emptyset$ equation. Present devault values are

   a. NSWPU = 4

    b. NSWPP = 5

    c. Remaining NSWP$\emptyset$ = 3

The general recommendation is that NSWPU should be greater than other velocities and scalars with the exception of P. NSWPP should be approximately twice NSWP$\emptyset$. If the problem of divergence arises, the generally recommended solution is the increase of NSWP$\emptyset$ and the decrease of URF$\emptyset$. The present author has found little effect results from the increase of NSWP$\emptyset$ with the exception of NSWPP. In problems that exhibit divergence, this may be increased to, say, NSWPP = 15 with some small effect on increase in stability.

17. CONTO.192 - ISTEP = n. The value n sets the axial location of the first node inside the inlet plane. The default value is 2.

18. CONTO.193 - JSTEP = n. The value n sets the radial location of the first node interior to the inlet wall. The default value is 14.

19. CONTRO.194 - JEXIT = n. The value n sets the radial location of first node interior to the exit nozzle wall at, or downstream of, the exit plane. The default value is 14.

20. CONTRO.199 - NJ = n. The value n sets the total number of nodes in the radial direction for which values are assigned or calculated. The default value is 24.

21. CONTO.205 - RLARGE = X. The value X is the radius of the combustor. The default value is 0.048768.

22. CONTRO.198 - INDCOS = n. The value n defines the coordinate system: n = 1 plane flows, n = 2 axisymmetric flows.

23. CONTRO.206 - ALTOT = X. The value X defines the length of the combustor from the inlet plane to the exit plane. The default value is 0.4064 m.

24. CONTRO.207 - ALTRAN = X. The value n defines the length of the combustor from the inlet plane to the transition point at which the area reduction of the nozzle commences. The default value is 0.381 m.

25. CONTRO.208 - ALINLT = X. The value X defines the length of the combustor from the inlet plane to the transition point where constant or maximum cross sectional area occurs. The default value is 0.

26. CONTRO.211 CONTRO.212 - NI = m NEXRAC = n. See note 4a, m and n are settings for coarse mesh.

27. CONTRO.214 - EPSX = X. The value X sets the geometric ratio for axial grid spacing increase/decrease for a coarse mesh. The default value is 1.11.

28. CONTRO.250 CONTRO.251 - NI = m NEXRAF = n. See note 4a, m and n are settings for fine mesh.

29. CONTRO.253 - EPSX = X. The value X sets the geometric ratio for axial grid spacing increase/decrease for a fine mesh. The default value is 1.102.

30. CONTRO.289 - $Y(j)$ = X. The value X is the radial location of the jth node in the radial direction.

31. CONTRO.331 - RINLT = $f(x(I))$. The function $f(x(I))$ is the definition of the inlet expansion profile. Present default is linear expansion. Alternate maximum radial nodes are located either side of defined profile.

32. CONTRO.366 - RTRAN = $f(X(I))$ - The function $f(x(I))$ is the definition of the nozzle contraction profile. Present default is linear contraction.

33. CONTRO.382 CONTRO.391 - INCALØ = .TRUE. Defining the value INCALØ to be TRUE/FALSE allows/inhibits the solution of the equation for variable ϕ.

27

34. CONTRO.397 CONTRO.400 - C_a = X. The value of constants in the k-ε turbulence model are defined here.

35. CONTRO.404 CONTRO.407 - PRØ = X. Turbulent Prandtl/Schmidt numbers are defined here. Default values are PRED = 1.22, PRTE = 1.0, PRH = 0.9, PRFR = 0.9.

36. CONTRO.409 - UIN = X. The value X is the average inlet velocity. This value is used in determining the initial conditions.

37. CONTROL.411 - TURBIN = X. The value of n is the turbulence intensity level at the input. The default value is 2%.

38. CONTRO.413 - ALAMDA = X. The value of internally defined length scales is X times the appropriate length. The initial boundary value for turbulence dissipation is determined from a length scale ALAMDA*COMBUSTOR DIAMETER.

39. CONTRO.415 - VISCOS = X. Laminar Viscosity is defined by X. The present default value is 17.11 x 10^{-6} kg/ms.

40. CONTRO.417 - PRANDT = X. Laminar Prandtl number is equal to X. The present default is 0.7.

41. CONTRO. 418 - TEMP = n. Gas inlet temperature is defined by X. The present default value is 248.5°K.

42. CONTRO.420 - HFU = X. The fuel heat of reaction is defined by X. The present default value is 0., representing the situation of no combustion.

43. CONTRO.422 - CPR = X. The quantity X represents the average specific heat at constant pressure for the gas mixture. The default value is 1004.

44. CONTRO.424 - WPR = X WOX = Y WFU = Z. The quantities X, Y, Z, represent the average molecular weights of combustion products, oxidizer, and gaseous fuel respectively. The default values are given for air as the oxidizer and for fuel simulated by argon.

45. CONTRO.428 - XI = X. The value X is the stochiometric oxidizer/fuel mass ratio.

46. CONTRO.432 - FUEL = X. The value X is the fuel mass fraction entering the combustor.

47. CONTRO.436 CONTRO.438 - PO = X IPREF = m JPREF = n. The value and location of the reference pressure is defined here. The values of m, n should be specified within the calculation domain. The default location is (2,2), near the intersection of symmetry axis and the inlet plane.

48. CONTRO.440 CONTRO.442 - IMON = m JMON = n SORMAX = X. The quantities m, n defined the node for which the monitor values of the three velocities, pressure and turbulence dissipation rate are printed at intervals determined by IPRINT. The value defined by SORMAX is the maximum accepted value for the sum of residual sources for convergence to occur.

49. CONTRO.477 - U(2,n) = X, TE(1,n) = Y, ED(1,n) = Z. Axial velocity, turbulence kinetic energy and turbulence dissipation rate at the inlet plane for all radial grid points are defined here.

50. CONTRO.507 - RHUB = X. The radius of the hub of the swirler is defined here. The hub radius is the region within which the swirl at the inlet plane is assumed to be solid body rotation.

51. CONTRO.534 - T(1,J) = X. Inlet plane temperature profile defined here equal to X.

52. CONTRO.570 - P(1,J) = X. The inlet plane pressure profile defined here equal to X. Default value is flat profile equal to reference pressure.

53. CONTRO.693 - Write (11) LIST. This statement writes to the restart tape a series of values to be used for normalization of dependent variables in the output plots. When rereading the restart tape, these values are read into the array DIMLES.

54. CONTRO.663, 664 CONTRO.740 CONTRO.754, 761 - URFØ = n. This section sets the underrelaxation factors. The default values should prove satisfactory for constant density flow. Some adjustment may be necessary for varying density flow. Decreasing the underrelaxation factor improves stability at the expense of convergence rate. For varying density flows, it is best to start with the fixed density solution as the initial condition. Another tip is to use a LO-HI-LO sequence for underrelaxation factors to bring the solution to quick stable convergence. Further work is needed in this area.

4. OPERATION OF STARRC POST PROCESSOR

The present STARRC Post Processor is named TCHPLT. The code will generate 3-D perspective views or 2-D plots of families of curves of the general variable Z versus the X and Y coordinates using the DISSPLA package.

To operate TCHPLT, it is necessary to first generate (IWRITE = .TRUE.) a restart file in STARRC. This file has the local file name TAPE11 and the normal procedure is to catalog this file at the end of a STARRC run. This file is then reattached as TAPE9 for TCHPLT.

TCHPLT is run in batch mode with the job control cards of Appendix A and a data deck constructed in the following manner. All data fields are 10 characters in width.

a. 3-Dimensional Plot

Card 1: (A10, I10, 6A10) 3DPLOT, DATAFILE, PLOT TITLE$ - The string 3DPLOT is left justified. The DATAFILE is a right justified integer defining the location of the file on the tape of the dependent variable (Table B-2) to be plotted on the Z axis. If datafile is a negative

number -k, all quantities on file k will be normalized by the values written on the file by STARRC (See 5.3.53). PLOT TITLE is a user-defined plot label and must be terminated with a $.

Card 2: (8I10) XDIM, FIRSTX, LASTX - These three quantities are right justified integers defining the dimension of the X array and the indices of the first and last X locations to be plotted respectively.

Card 3: (8I10) YDIM, FIRSTY, LASTY - These three quantities are right justified integers defining the dimension of the Y array and the indices of the first and last Y location to be plotted respectively.

Card 4: (2E10.0, 6A10) XAXIS, XNORM, XLABEL$

Card 5: (2E10.0, 6A10) YAXIS, YNORM, YLABEL$

Card 6: (2E10.0, 6A10) ZAXIS, ZNORM, ZLABEL$ - The values XAXIS, YAXIS, ZAXIS, define the proportional lengths of the respective AXES. The values XNORM, YNORM, ZNORM may be any positive real number and are normalization factors for the appropriate axes. The ALPHA strings XLABEL, YLABEL, ZLABEL provide the labels for the appropriate axes and must be terminated by $.

Card 7: BLANK CARD

Card 8: (2E10.0, 6A10) PHI, THETA - PHI and THETA define the view angle. PHI is the angle positive anticlockwise from XAXIS, THETA is the angle positive when the observer is above the XY-plane.

b. Two-Dimensional Plots

Card 1: (A10, I10, 6A10) 2DLABEL, DATAFILE, PLOT TITLE$ - The alpha string 2DLABEL determines the type of plots according to the following table.

31

LABEL	PLOT
2DYVSX	PLOTS of Y vs X for constant Z
2DZVSX	PLOTS of Z vs X for constant Y
2DZVSY	PLOTS of Z vs Y for constant X

The value of Z is the value of the variable defined by the DATAFILE. Comments for DATAFILE and PLOT TITLE for 3-dimensional plots apply.

Cards 2, 3, 4, 5, 6: These cards are identical to those used in 3-D plots with the exception that the values XAXIS, YAXIS, ZAXIS now define the actual length of the plot AXES in inches.

Card 7: (8E10.0) XMIN, DELX, YMIN, DELY - This card sets the plot scaling. A blank card will invoke automatic scaling. To predetermine the scales, set XMIN and YMIN to minimum value on X and Y axes respectively and DELX and DELY to the required scale, in units per inch of plot for X and Y axes respectively.

Card 8: (8I10) N - The quantity N is a right justified integer defining the number of curves in the family to be plotted.

Card 9: (8I10) α_1, α_2, α_3, α_n - Card 8 contains N values, one for each requested curve in the family plotted. The term α_i defines the value of the parameter held constant for the ith curve.

Card 9 to 9+N: (E10.0, 2I10) S(I), JJS(I), IIS(I) - Cards 9 to 9+N contain parameters for the N requested curves. The term S(I) sets the value of the parameter held constant for the ith curve. The term JJS(I) sets the symbol to be used in plotting. JJS(I) may have a value between 0 and 15. The term IIS(I) determines whether symbols are plotted according to the following table

ISYM = -1	point symbols only
ISYM = 0	connecting lines only
ISYM = +1	point symbols and connecting lines

32

c. Termination of Data Deck

The data deck must be terminated with a card containing the left justified alpha string DONE.

5. OPERATIONAL EXPERIENCE WITH STARRC CODE

This section outlines a number of problems encountered with the STARRC Code and possible solutions.

a. Iteration Control

The iteration process is monitored by comparison of the absolute values of the residual sources of mass and preselected dependent variables in the flowfield with a present value, SORMAX, representing the maximum source. Iteration is terminated when the largest residual source is less than SORMAX, a divergence criteria is invoked, or a preset number of iterations is reached. In general, this procedure has worked well and the approach is particularly suited for production runs from restart tapes where an approximate idea exists of the number of iterations needed for solution.

When a new case is being modelled for the first time, the procedure is not so successful. With this type of problem, interactive programming is preferred to allow problem debugging, monitoring of convergence, and alteration of quantities such as underelaxation factors as required. Unfortunately, core memory restrictions prevent this on the present computer system.

A proposed solution is to remove the iteration number limit and instead to relay on job time limit for maximum limit to the number of iterations. After each iteration, the execution time (from subroutine second (t) on CDC system) is compared with the job time limit and at a preset difference the restart file is generated and the execution terminated. This will prevent the loss of the restart file that presently

occurs if job time limit is reached before convergence or iteration
limit and will allow the batch submission of a number of short time jobs
to hasten debugging and monitor convergence.

b. Convergence Control

The problems of convergence are essentially those of excessive
slowness to converge, divergence, or convergence with lack of conservation
of variables that require conservation. The Fortran variables which
influence the iteration behavior are the number of update sweeps NSWPØ
and the under-relaxation factors URFØ. As stated earlier, if divergence
occurs, the remedy generally lies in increasing the former (especially
for pressure) and decreasing the latter. For excessively slow convergence,
the reverse applies. Note, however, that increasing the number of grid
points also tends to increase the number of iterations required for
convergence. In general, the present values of NSWPØ and the routine
adapted from STARPIC for varying URFØ have been found adequate for
constant density flows.

The solution is not so clear for varying density flows. For many
problems convergence is still obtained simply by increasing NSWPP to 15,
reducing URFP to 0.5 and URFRHO to 0.2, rather starting the varying density
solution with initial conditions derived from a wholly or partly converged
constant density solution. The reasons that this procedure is not always
successful are inherent in the method in which the density variations
have been introduced. Consider the effect of the various logic switches.
If IROTEM is set .TRUE., local density is calculated from the equation
of state and rather than assigned a fixed initial value. Variations in
local absolute pressure will alter the local density. If INCALFR is set
.TRUE., a second species is transported and local density variations may
also occur due to variations in concentration of a gas of different
molecular weight. If INCALH is set .TRUE., local variations in temperature
and, through the equation of state, density may occur since temperature
is now calculated from local enthalpy rather than assigned a fixed value.
If INMACH is set .FALSE. and INCALH is set .TRUE., the static enthalpy is

calculated and temperature variations will occur only if heat is released due to chemical reaction (INREAC = .TRUE.). If however, INMACH is set .TRUE. and INCALH is set .TRUE., stagnation enthalpy is calculated and variations in local kinetic energy will be reflected in variations in temperature, density, and pressure.

Under all of the above conditions, variations in density arise only through the equation of state in the PROP subroutine. The equation for calculation of pressure has not been altered. Consequently, the solution proceeds in the following way.

(1) With an assumed pressure p^* and density ρ^* initial values of axial and radial velocities u^* and v^* are calculated.

(2) Using the above values and the equations of continuity of mass and momentum, corrected values u, v, and p are derived $u = u^* + u'$, $v = v^* + v'$, $p = p^* + p'$.

(3) Using the new values for p and the latest value of temperature, a new value for ρ is defined from the equation of state.

As a result of step (3) above, local continuity will no longer occur and the solution for pressure and density tends to be explicit rather than implicit with possible divergence. If the value of pressure used in the calculation of the equation of state is large compared to the pressure correction terms, density correction terms are small and convergence results. Otherwise, the solution will tend to diverge. Increasing the grid spacing changed a diverged solution to a convergent solution in one test case. This procedure is not always acceptable and the long term solution is to alter the algorithm for calculation of pressure correction terms to include the effect of variations in density.

If the solution procedure stagnates or converges without conservations of quantities that should be conserved, present experience suggests that this nearly always results from an inconsistent set of boundary conditions.

35

Krishnamurthy (Reference 17) reports that a coarse grid mesh can also lend to an absence of mass conservation for the diffusion of a second species.

c. Accuracy of Solution

The accuracy with which the differential equations are being solved is dependent on a number of factors, one of which is grid size. If increases in mesh density produce no significant changes in the dependent variables at locations in the flow of interest to the modeller, the grid configuration may be considered as adequate. The grid densities used in the following case studies may be used as guides.

It is interesting to note here the problem that occurs in the specification of the step boundary condition for both sloping inlets and nozzles. The problem occurs if a step has several points in the horizontal direction and is manifested as an oscillating rather than steady change in the static pressure along the wall. This problem is illustrated in Figure 5 which shows the configuration of a stepped nozzle and indicates the experimentally computed static pressures (relative to the flow reference pressure). It is doubtful if these variations have any significant effect on the flowfield and it is assumed that the problem is numerical. Some further investigation of the boundary conditions for the solution of the pressure correction equation might prove helpful. The simulation of the nozzle boundary by a nonorthogonal grid (thus eliminating the present staircase procedure) should remove this problem.

To a large extent, assessment of the accuracy of the modelling procedure for other than simple pipe flows suffers from a dearth of data from well defined experimental programs that could be used as a baseline for comparison purposes. Similarly, predictions of flows for combustor geometries is often hampered by lack of knowledge of boundary values. Several experimental programs are planned to correct these deficiencies.

Three case studies follow that illustrate the use of the program at the present stage of development.
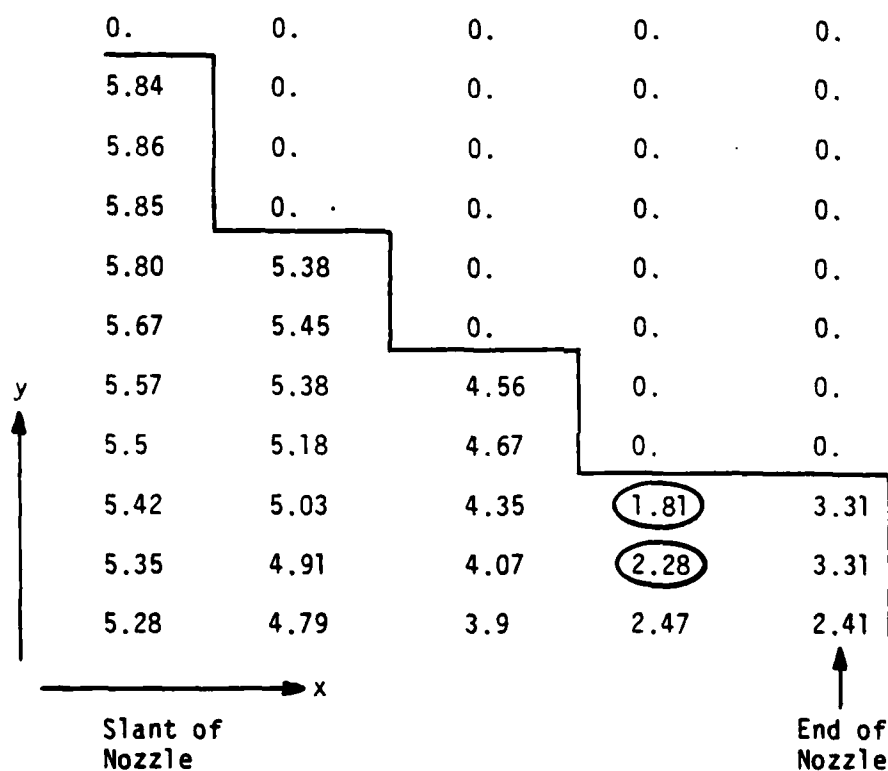
```
0.        0.        0.        0.        0.
 ┌─────────┐
5.84  │    0.        0.        0.        0.
      │
5.86  │    0.        0.        0.        0.
      │
5.85  │    0. ·      0.        0.        0.
      └─────────┐
5.80       5.38  │   0.        0.        0.
                 │
5.67       5.45  │   0.        0.        0.
                 └─────────┐
5.57       5.38       4.56 │  0.        0.
                           │
5.5        5.18       4.67 │  0.        0.
                           └──────────────────────┐
5.42       5.03       4.35    ⟨1.81⟩    3.31
5.35       4.91       4.07    ⟨2.28⟩    3.31
5.28       4.79       3.9     2.47      2.41
```

y ↑

x →

Slant of   End of
Nozzle   Nozzle

Figure 5. Static Pressures (kP) Relative to Reference
           Pressure Near Wall of Nozzle Simulation

Note present discrepancy (circled) in simulation of
pressure near wall.

6. CASE STUDIES

Case 1   Model Verification for Axisymmetric Dump Combustor Geometry

Though a number of research programs are attempting to remedy the situation, at present one of the most comprehensive investigations of the turbulent flow in an axisymmetric dump combustor geometry is that of Drewry (Reference 15) who has investigated cold flow conditions employing surface flow visualization, pressure probing and on-line gas sampling with a quadrupole mass spectrometer. This case study reports the modelling of one of Drewry's configurations illustrated in Figure 6. An array of eight circumferential fuel injection ports located 63.5 mm upstream of the dump plane was connected to a separate gas (fuel) feed system. Measurements included wall static pressure, static and total pressure traverses and concentration measurements made when argon was injected through the fuel ports. It is worth noting that the concentration measurements were performed in a horizontal plane (two fuel injectors are in this plane) and no check was made on the axis of symmetry of the measured fuel distribution.

Drewry's first traverse station for both velocity and concentration was made at 2.54 mmm from the dump plane. This traverse was used to set the initial conditions of velocity and fuel mass fraction. A uniform inlet static pressure profile and 2% turbulence intensity were assumed. The combustor was modelled by a 48 x 24 variably spaced grid for the variable density solution and a 96 x 24 variably spaced grid for the fixed density solution. Rapid convergence occurred for the fixed density solution. The variable density solution was more sensitive to initial conditions and chosen underrelaxation factors and convergence was not achieved for the 96 x 24 grid.

Measured and predicted values for the wall static pressure, velocity distribution and fuel mass fraction are shown in Figures 7, 8, and 9. Note that excellent agreement occurs between predicted and measured values of wall pressure and velocity. The difference between the model and the
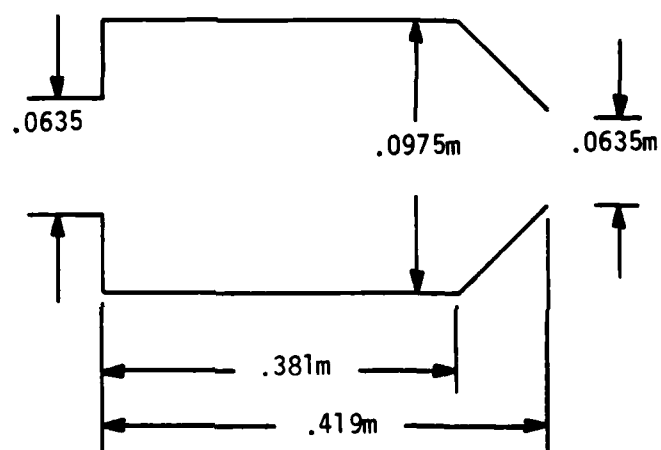
Figure 6.   Configuration of Drewry Modelled in Case 1 and 2
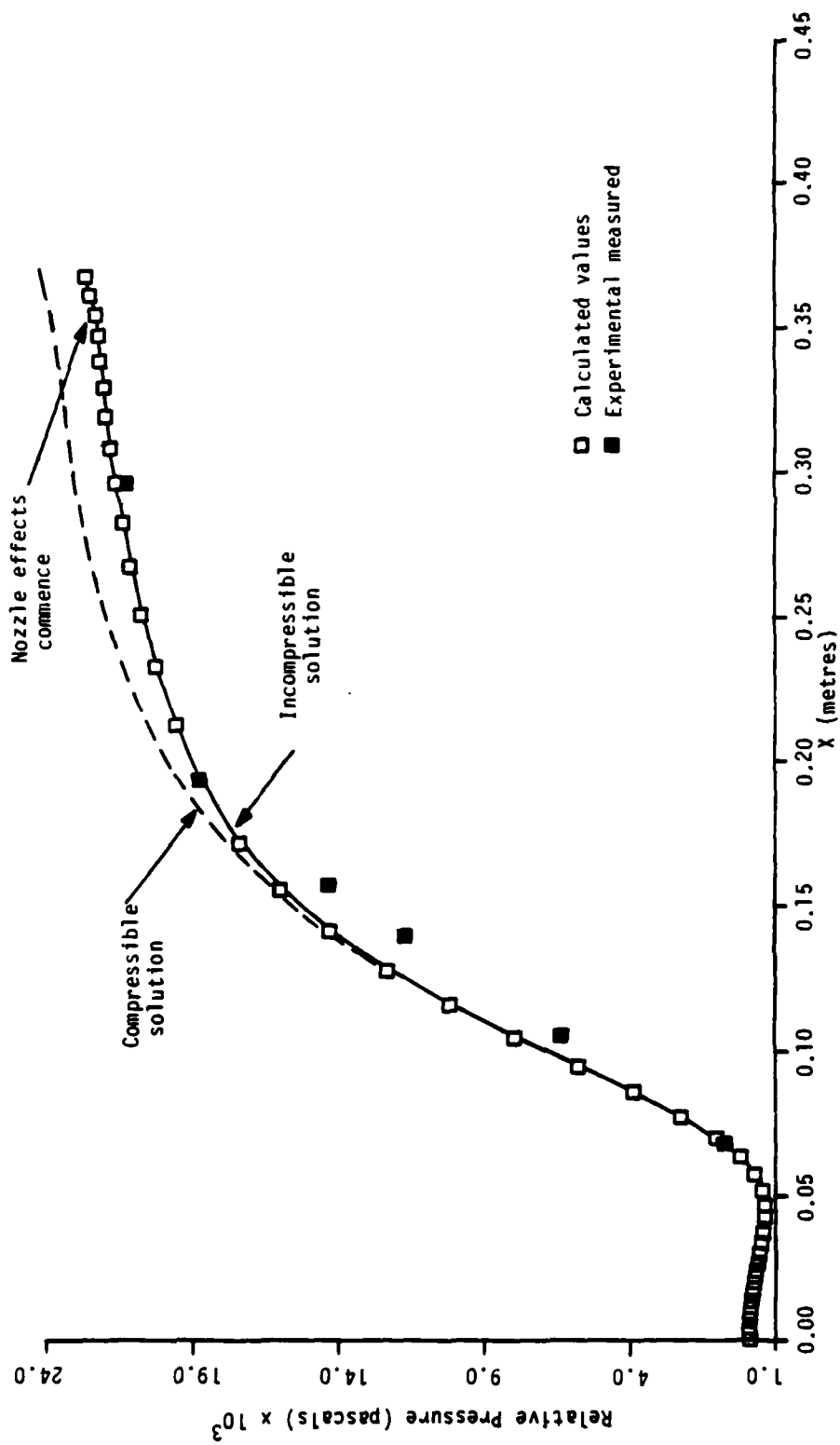
Figure 7. Wall Static Pressure Relative to Static Pressure
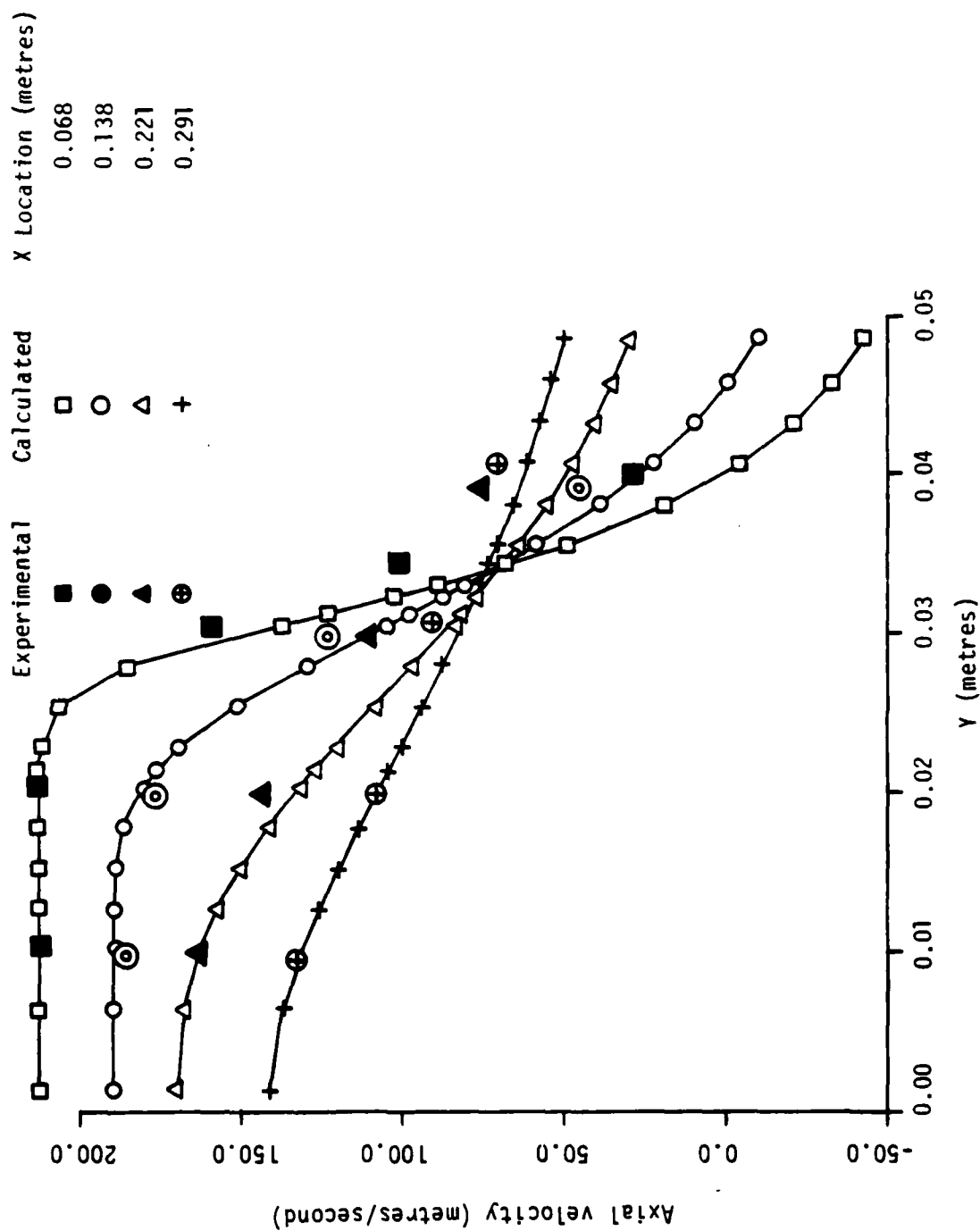
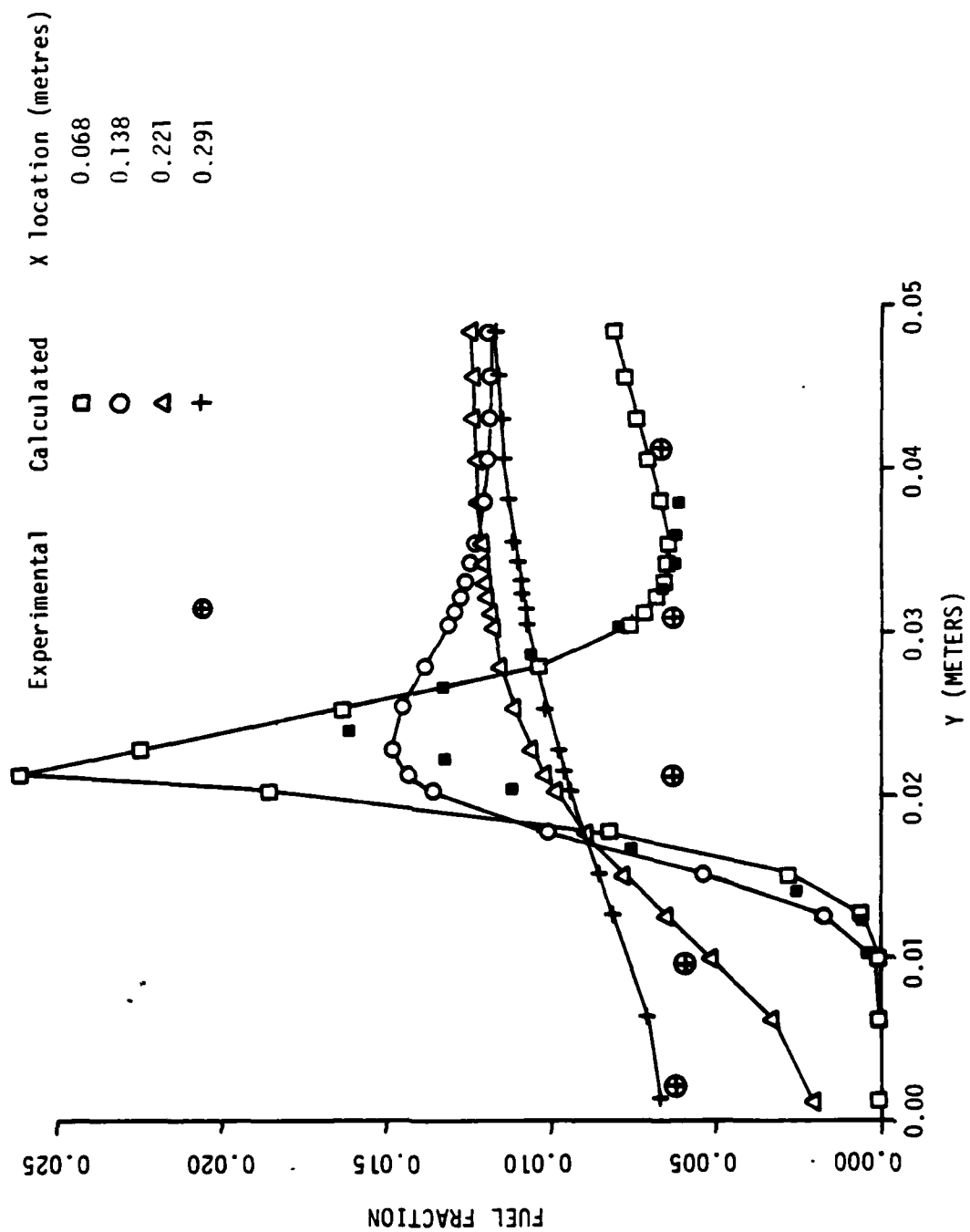Figure 8. Axial Velocity Distribution

Figure 9. Fuel Mass Fraction

experiment for the velocity in the region of the wall can be attributed
to the fact that Drewry was using pitot probes in a highly turbulent
region of the flow and that the model is using stationary axisymmetric
flow while the experiments observed that this was not the true case. Note
that the coarser grid variable density model gave slightly better
predictions of velocity and fuel mass fraction and slightly worse
predictions of wall pressure than the finer grid fixed density model.
The model needs to be refined to enable use of variable density without
the special care presently required to obtain convergence.

The fuel distribution shows good qualitative trends but there is
disagreement between the actual and predicted values. The normalized
profiles would show considerably better agreement. The difference can be
attributed to the fact that the fuel distribution was not axisymmetric
prior to the dump plane and that the input profile used had higher average
than the actual average value (since it was in the plane of 2 fuel
injectors as previously indicated). The present plan is to further extend
the verification of the computer model by comparison of other dump
configurations of Drewry (Reference 15) and of Boray (Reference 18).

Case Study 2 - Effect on Fuel Distribution of Addition of Swirl

Buckley et al (Reference 16) have shown that significant reduction in
combustion chamber length and total pressure loss can be achieved by the
introduction of swirl to the flow upstream of the dump plane. This case
study investigates the distribution of the total fuel throughout the
combustor chamber in the flow conditions of case 1 when swirl is introduced.
Three swirl profiles (Forced vortex or solid body rotation, Flat swirl
or fixed angle, and Free vortex) were investigated.

Results are presented for nominal swirl number 0.4 for the extremes of
Forced Vortex ($W \sim r$) and Free Vortex ($W \sim \frac{1}{r}$) swirl - the Flat swirl results
lie between these extremes.

For all profiles, the inlet dump plane contained a region of forced
vortex (solid body rotation) from the centerline to .1875 Rstep. This
represented the hub used in the swirlers produced by Buckley (Reference 16).
Calculations were made for 48 x 24 grid variable density flow. Figure 10
shows the fuel mass fraction distribution throughout the combustor for
no swirl, forced vortex and free vortex swirl.

Note that the free vortex profile produces an evenly distributed fuel
mass fraction more rapidly than the forced vortex. Qualitatively, these
results show agreement with the experiments of Buckley who found that
the swirl profiles could be ranked Free vortex, Constant angle, or Forced
vortex in order of decreasing combustion efficiency. Care must be taken
not to extrapolate this comparison too far since even the forced swirl
case gave a better combustion efficiency (Reference 16) than no swirl
while this was not the case for the computer predictions of the fuel
mass fraction distribution. The reason for the variation with swirl
profile lies principally in the effect of the swirl pattern on the
central and peripheral recirculation zones. It should be noted that
swirl profile is only one of several factors that may effect these
recirculation zones. Other factors are reported by Rhode and Lilley
(Reference 19).

Several authors (References 19-22) have attempted to model swirl in
combustor configurations and have encountered problems with the prediction
of turbulence. It is prudent therefore to recommend further experiments
involving swirl with the measurement of turbulence and species in both
hot and cold flows. These experiments are under consideration at
AFWAL/PORT.

Case 3 - Modifications to Outer Wall

This case study relates to the alteration of combustor outer wall
geometry in an effort to reduce the total pressure loss through the
combustor. The initial configuration is shown in Figure 11. The
combustor has a shorter L/D than that of Drewry and contains an elliptical
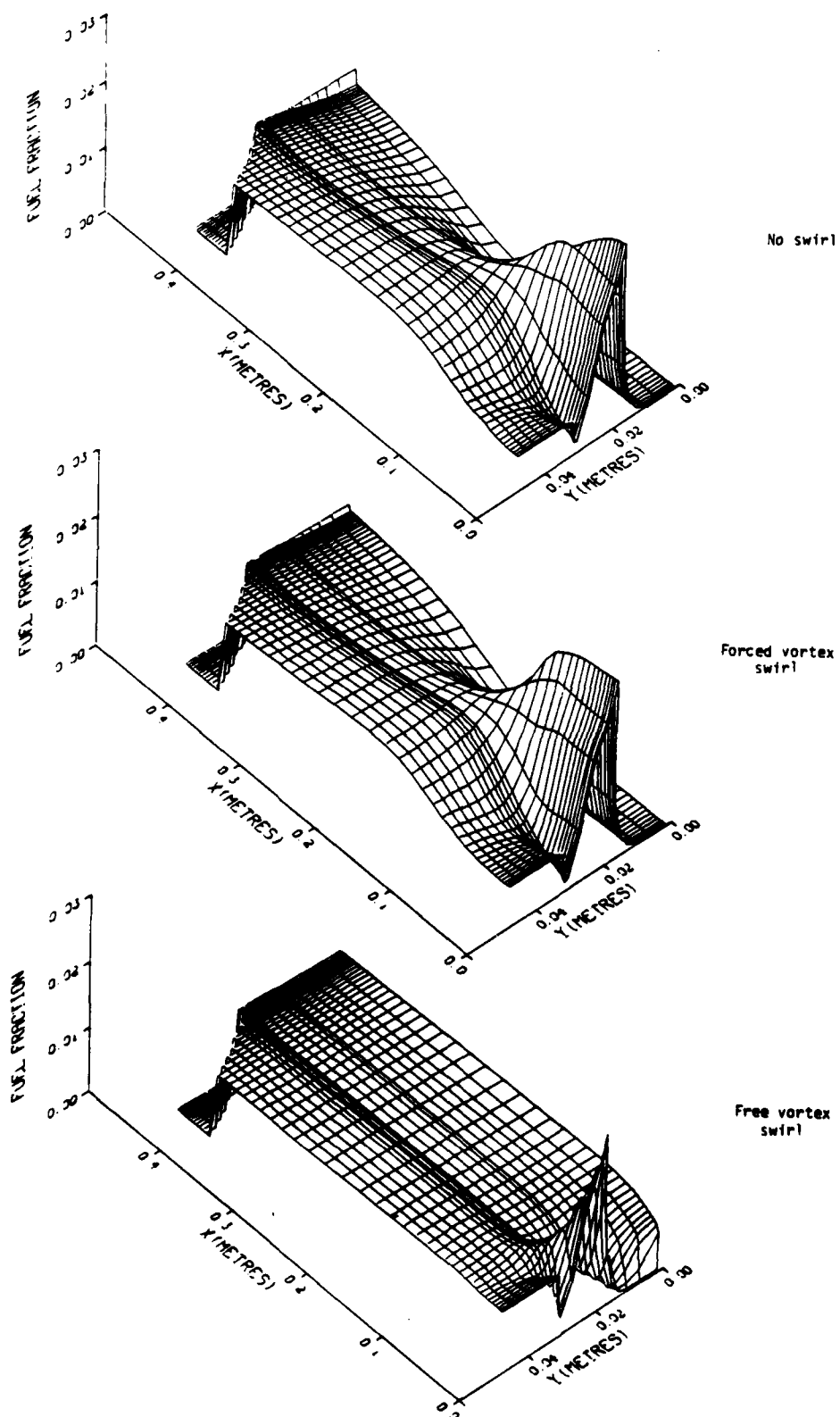rather than a straight converging nozzle.

No swirl

Forced vortex
swirl

Free vortex
swirl

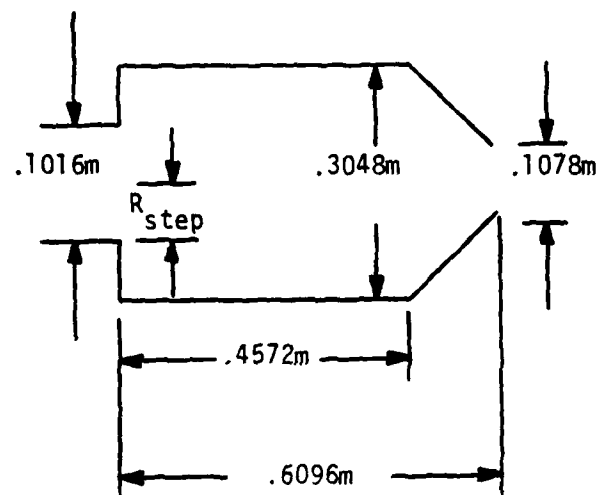Figure 10. Fuel Mass Fraction in Combustor

45

Figure 11. Configuration of Parker et al Modelled in Case 3

The proposed configuration change suggested by Buckley was to utilize a sloping wall rather than a dump, thus eliminating the peripheral recirculation zone and hopefully reducing total pressure loss. The flame stabilization was to be provided by a swirl induced central recirculation zone. The combustor was modelled for the flow of cold air (no fuel) using a 48 x 24 variably spaced grid and the variable density solution. Free vortex swirl (nominal swirl number 0.4, 0.6) was introduced for the proposed configuration change of 45° sloping inlet and constant angle inlet to the start of the nozzle. The flowfield streamlines for the latter geometry and for a dump combustor for the case of no swirl and nominal swirl number 0.4 are depicted in Figure 11. Examination of Figure 11 reveals that the peripheral recirculation zone is removed by the introduction of the sloping wall at the expense of a reduction in size of the central recirculation zone. Originally it was hoped that the central recirculation zone would increase in size with the alteration in geometry. This reduction in the central recirculation zone could lead to flame stability problems at reasonable swirl numbers and consequently no combustion experiments were performed with the altered geometry.

An interesting proposed follow-on case study would be to run the code with the inlet fuel distribution of Drewry and observe the effect on the fuel distribution in cold flow of these configuration changes. Experimental measurement could be included with those mentioned in case study 2 to see if the central recirculation zone is actually decreased and what effect this has on the fuel distribution. The results of these numerical and experimental studies would be a better guide than the results presently available to the wisdom of proceeding with combustion experiments.
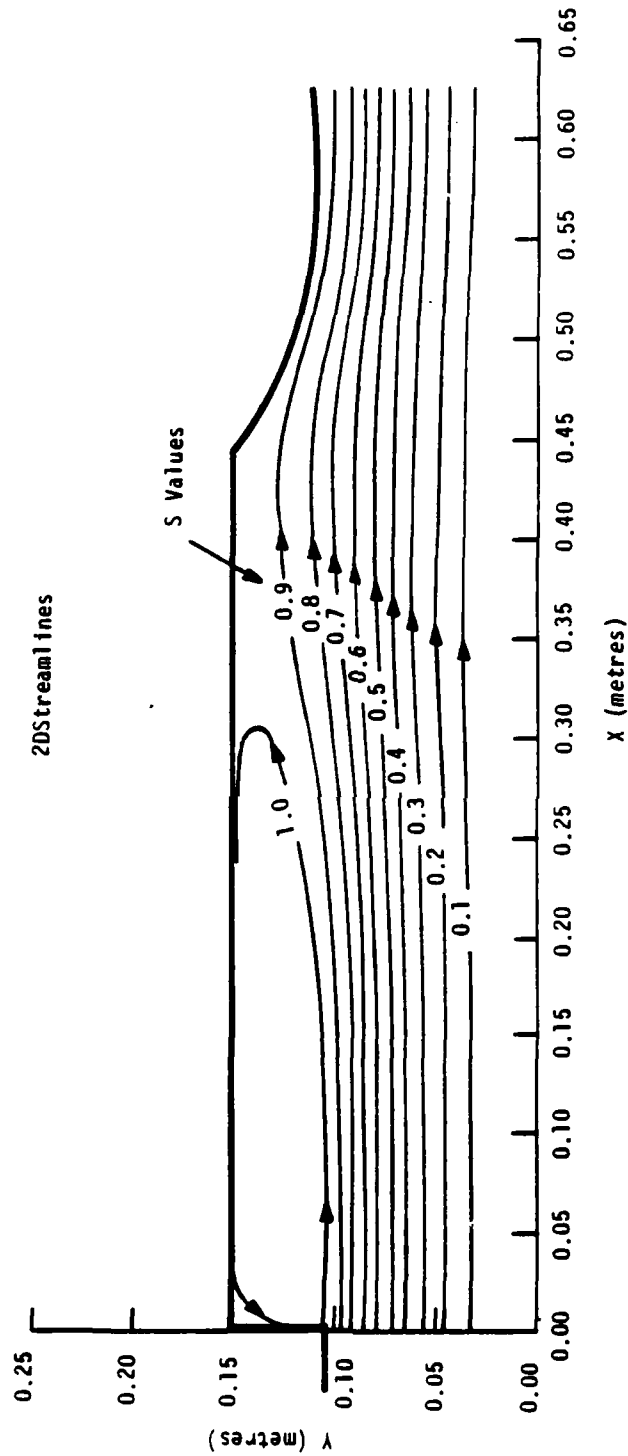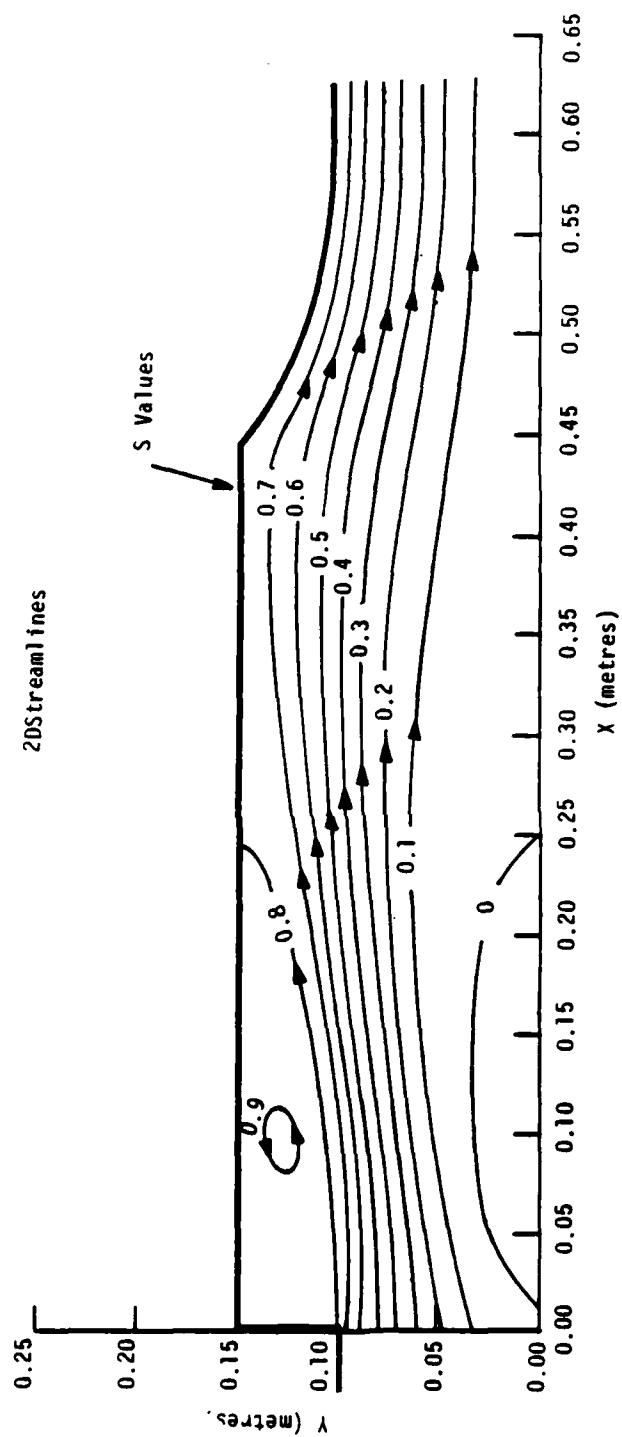
2DStreamlines

Figure 12a. Dump Combustor, No Swirl

2DStreamlines

Figure 12b. Dump Combustor with Swirl

Figure 12c. Sloping Inlet, No Swirl

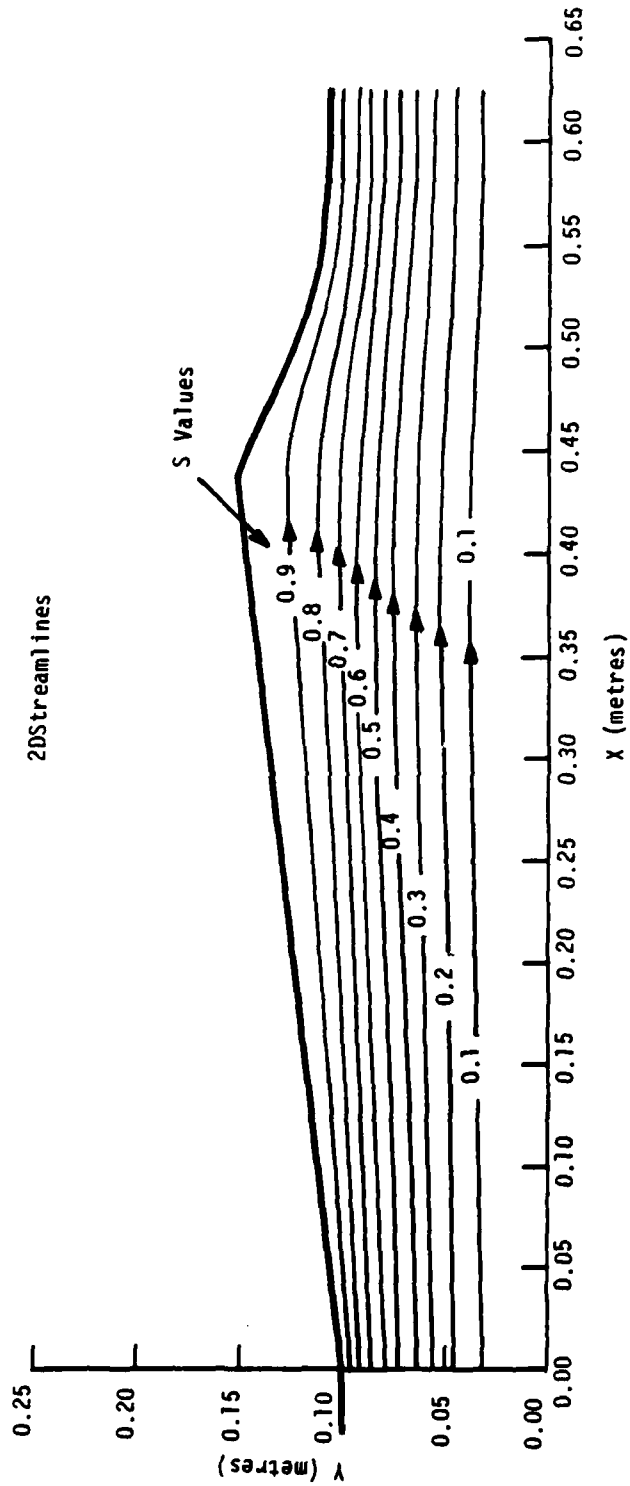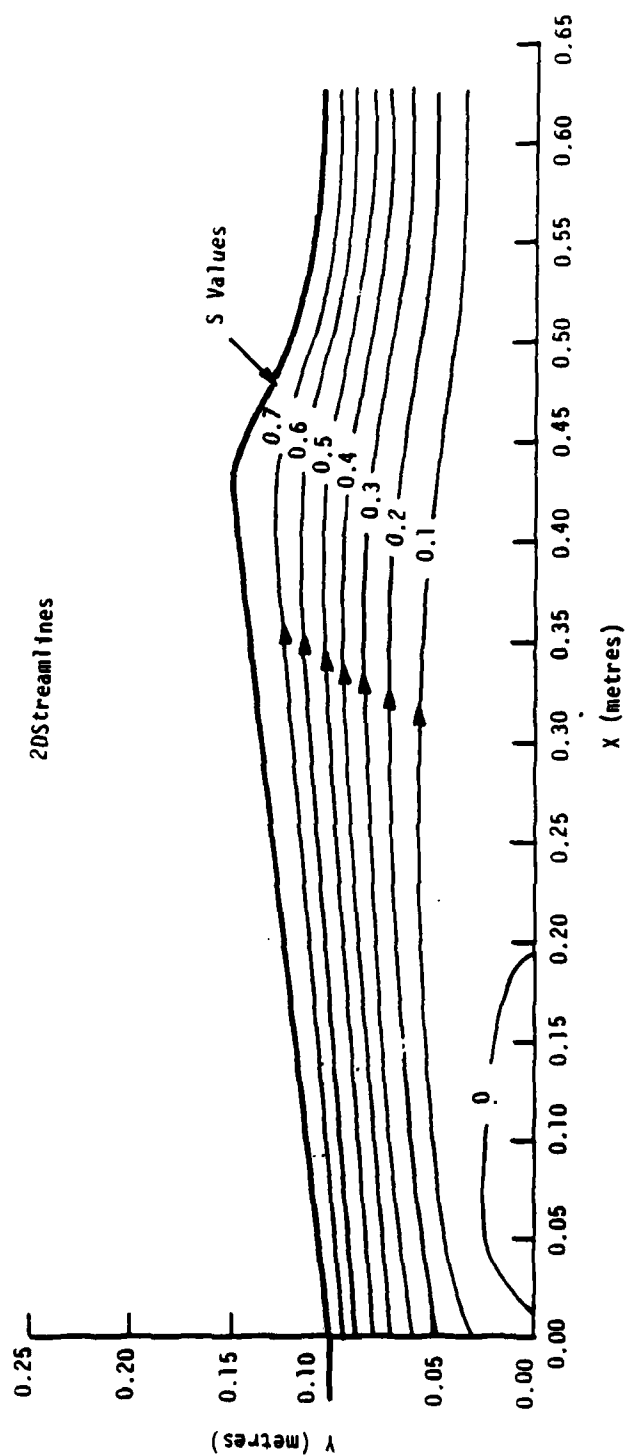2DStreamlines

Figure 12d. Sloping Inlet, Swirl

SECTION VI

THE NASA-GARRET CODE

1. INTRODUCTION

The plan for the adaptation of this code to ramjet configurations proposes a number of separate tasks as outlined below.

a. Adapt code for operation on ASD CDC computer.

b. Adapt code for operation on AFWL Kirtland CRAY computer.

c. Adapt code for side inlet combustor with no dome inlet flow. Model this configuration for water flow and compare results with water tunnel measurements.

d. Add a dome inlet flow to the model of case 3 to simulate the presence of the gas generator jet in the combustor. Model the configuration for water flow and compare results with that of the water tunnel experiments and the results predicted by a 3-D isothermal flow code capable of finer grid resolution than the NASA-Garrett code (Section IV).

e. Model the flow of cold air and compare results with those obtained in gas sampling experiments and Laser Doppler Anemometer measurements and the results predicted by a 3-D isothermal flow code capable of finer grid resolution than the NASA-Garrett code (Section IV).

f. Model the combustion of Hydrocarbon fuel utilizing geometries presently under experimental evaluation. Compare results with experiments.

g. Perform experiments with the code involving variations of present experimental parameters. This may involve variations in geometry, inlet flow conditions, and the nature of the fuel.

2. PROGRESS TO DATE

Tasks a, b, c have been proceeding simultaneously and are reported collectively. The principal reason for adapting the code to the CRAY

computer is to make use of its superior memory storage and speed capabilities. Approximately an order of magnitude decrease in the runtime can be achieved without major changes in the code logic by running the code on the CRAY vector processor rather than the ASD CDC machine. The present system for submission of jobs to the CRAY from ASD is not an acceptable procedure for debugging of programs because of limited access availability and slow response. Consequently, the best procedure is to debug codes on the ASD machine and to limit CRAY operations to production runs. Job submission to the CRAY may include the program and/or data as input or may retrieve these from the mass storage system at Kirtland.

Operation of the code on the ASD CDC computer is straightforward. The code must be compiled in Fortran 5 because of the nature of the format statements. The principal limitation to effective operation is restriction on memory size. The supplied three dimensional code requires an execution file length of $367,200_8$ words for a non-optimized array structure suitable for a 15 x 15 x 7 grid. This requirement is too close to the imposed third shift limit of $377,000_8$ words to allow loading of the debug routines. Consequently, a general update correction deck named "MYCOMMONBLOCKUPDATER" has been constructed to allow optimum array construction for the desired grid size. "MYCOMMONBLOCKUPDATER" is edited according to instructions supplied in Appendix B and the resultant file, for example "COMBUG", is applied as an UPDATE correction deck to the "THREEDPROGRAMLIBRARY". "COMBUG" will allow the construction of a 15 x 7 x 7 grid and when loaded with debug options requires $313,400_8$ words of memory. Further increases in grid size may be achieved by removing the calculations of Nox emissions from the program. Modifications to the code allowing the simulation of the side entry combustor are included in the update correction deck "SIDEINUPDATER". The procedure has been to simulate the side inlet by altering the boundary conditions for the locations designated as radial injection points in Reference 14 to provide the injection velocity with a radial and an axial component. This procedure is relatively unsophisticated and may need to be improved. The remainder of the correction deck is to allow for the conditions of

zero fuel, zero dome inlet flow, and constant density flow as required for the comparison with the water tunnel experiments. It should also be noted that the following corrections should be made to the present card input deck:

a. Card 20, fuel properties must contain non-zero values even if no fuel is input.

b. Card 28, last three fields should read TCYLW, TINLW, TLIP.

c. Card 26, description of dome inlet. JSW1, JSW2 must contain values greater than 1 even if no flow through this inlet.

d. Card 27, temperature at the dome inlet must not be set at zero even if no flow through this inlet.

Further modification to this deck are being made to enhance "user friendliness" of this code. It will also be necessary to supply fuel injection at the side inlets so that the combustion experiments of task 6 may be simulated.

SECTION VII

CONCLUSION AND FUTURE WORK

The current design practice for simple gas turbine and industrial combustor geometries employs computer codes in preference to experimentation for predicting parametric trends. Future development of these codes will obviously lead to wider application for more complex flows.

The present work has illustrated that the codes presently under development for gas turbine combustors can also be applied to ramjet combustor configurations. Qualitative trends can be predicted by present codes and the determination of the quantitative accuracy of the codes is somewhat limited by the lack of well defined experimental data.

Future work in the ramjet modelling area may proceed along a number of paths. The following tasks can be clearly identified.

1. Further refinement of the present 2-D model and the expansion of the model to include reaction kinetics in order to obtain a more realistic model of the ramjet dump combustion process. Further numerical simulations and experimental measurements are needed to determine the limits of applicability of the present modelling procedure. Possible experiments are suggested in Section V.6.

2. A continuation of the task of adapting the 3-D codes to the Ramjet configurations of Figure 1d.

3. The adaptation of the codes to a more user friendly format including such features as grid generation and initial condition preprocessor, iteration diagnostics and graphic displays. The generation of a data base of solutions on restart tapes to form initial conditions for future similar problems would be a useful procedure.

4. The modification of the codes to include such operational improvements as mesh imbedding, adaptive grids, models of sloping boundaries and dynamic variation of underrelaxation factors.

5. Improvement in models of physical phenomena. Consideration should be given to higher order closure models presently being included in some codes. The use of solid fuels may necessitate the derivation of combustion reaction models peculiar to the ramjet area.

APPENDIX A

Typical TCHPLT Job Control Deck

```
JOB, T25, IO50, CM 155000.  PXXXXXX.
ATTACH, TCHPLT, STARRCPLOTTER, ID = HARCH.
ATTACH, TAPE9, STARRCWRITEFILE, ID = XXXXX.
REQUEST, TAPE99, *Q.
ATTACH, DISSPLA8, ID = A780283, SN = ASD.
LIBRARY, DISSPLA.
FTN, I = TCHPLT.
MODE, 1.
LGO.
ATTACH, UNP 1038, ID = LIBRARY, SN = ASD.
UNPLO38.
ROUTE, TAPE99, DC = PU, TID = XX, ST = CSA, FC = NG.
*EOR
DATA
*END OF JOB
```

Note that the FC parameter controls the plot paper according to the following format:

NG	Narrow Grid
WG	Wide Grid
NP	Narrow Plain
WP	Wide Plain

APPENDIX B

Editing of MYCOMMONBLOCKUPDATER

An update deck that will modify the library deck "THREEDPROGRAMLIBRARY"
to enable calculations for a grid L, M, N can be produced by editing the
general correction deck "MYCOMMONBLOCKUPDATER" in the following manner:

REPLACE		BY	
	NXYZ		L*M*N
	7*XYZ		7*L*M*N
	NX,NY,NZ		L,M,N
	NX,NY		L,M
	NXY		L*M
	M2XYZ		(L-2)*(M-2)*(N-2)
	XYMZ		(L-2)*(M-2)
	NX		L
	NY		M
	NZ		N
	1XYZP1		1*L*M*N+1
	2XYZP1		2*L*M*N+1
	3XYZP1		3*L*M*N+1
	4XYZP1		4*L*M*N+1
	5XYZP1		5*L*M*N+1
	6XYZP1		6*L*M*N+1

TABLE B-1

**THE FORM OF THE COMPONENTS OF THE LINEARIZED SOURCE TERM*,
THE CELL VOLUME INTEGRAL $_V\int S_\phi dV = S_p^\phi \phi_p + S_U^\phi$
OF EQ. (1) FOR 2-D AXISYMMETRIC ISOTHERMAL FLOW**

ϕ	Γ_ϕ	S_p^ϕ/V	S_U^ϕ/V
1	0	0	0
u	μ	0	$S^u - \frac{\partial P}{\partial x}$
v	μ	$-2\frac{\mu}{r^2}$	$S^v + \frac{\rho w^2}{r} - \frac{\partial P}{\partial r}$
w	μ	0	$-\frac{\rho vw}{r} - \frac{w}{r^2}\frac{\partial}{\partial r}(r\mu)$
k	$\mu/\sigma k$	$-C_\mu C_D \rho^2 k/\mu$	G
ϵ	μ/σ_ϵ	$-C_2\rho\epsilon/k$	$C_1 C_\mu G\rho k/\mu$

In this table certain quantities are defined as follows:

$$S^u = \frac{\partial}{\partial x}\left(\mu\frac{\partial u}{\partial x}\right) + \frac{1}{r}\frac{\partial}{\partial r}\left(r\mu\frac{\partial v}{\partial x}\right)$$

*In this table, V stands for the cell control volume and $\mu = \mu_{eff}$.

$$S^V = \frac{\partial}{\partial x} \left(\mu \frac{\partial u}{\partial r} \right) + \frac{1}{r} \frac{\partial}{\partial r} \left(r\mu \frac{\partial v}{\partial r} \right)$$

$$G = \mu \left[2 \left\{ \left(\frac{\partial u}{\partial x} \right)^2 + \left(\frac{\partial v}{\partial r} \right)^2 + \left(\frac{v}{r} \right)^2 \right\} + \left(\frac{\partial u}{\partial r} + \frac{\partial v}{\partial x} \right)^2 \right.$$

$$\left. + \left\{ r \frac{\partial}{\partial r} \left(\frac{w}{r} \right) \right\}^2 + \left(\frac{\partial w}{\partial x} \right)^2 \right]$$

TABLE B-2

FILE NUMBERS FOR TCHPLT ROUTINE
LFS IS THE SWIRL LOOP INDEX

File Number	Dependent Variable
$(LFS-1)*13 + 1$	Axial Velocity U
$(LFS-1)*13 + 2$	Radial Velocity V
$(LFS-1)*13 + 3$	Swirl Velocity W
$(LFS-1)*13 + 4$	Static Pressure P
$(LFS-1)*13 + 5$	Turbulence Kinetic Energy TE
$(LFS-1)*13 + 6$	Turbulence Dissipation ED
$(LFS-1)*13 + 7$	Effective Viscosity VIS
$(LFS-1)*13 + 8$	Stream Function STFN
$(LFS-1)*13 + 9$	Mixture (total fuel) Fraction FR
$(LFS-1)*13 + 10$	Oxidizer Mass Fraction OX
$(LFS-1)*13 + 11$	Fuel Mass Fraction FU
$(LFS-1)*13 + 12$	Enthalpy H
$(LFS-1)*13 + 13$	Density ρ

REFERENCES

1. D. C. Lilley, Prospects for Computer Modelling in Ramjet Combustors. AIAA Paper No. 80-1189, Hartford, Connecticut, June 30-July 2, 1980.

2. P. T. Harsha and R. B. Edelman, Application of Modular Modelling to Ramjet Performance Prediction, AIAA Paper 78-944, Las Vegas, Nev., July 25-27, 1978.

3. C. E. Peters, Turbulent Mixing and Burning of Coaxial Streams Inside a Duct of Arbitrary Shape, TR-68-270, Arnold Engineering Development Center, January 1969.

4. D. C. Hammond, Jr. and A. M. Mellor, A Preliminary Investigation of Gas Turbine Combustor Modelling, Combustion Science and Technology, Vol. 2, 1970, p. 67.

5. R. S. Fletcher and J. B. Heywood, A Model for Nitric Oxide Emissions from Gas Turbine Engines. AIAA Paper 71-123, 1971.

6. J. Swithenbank, I. Poll, M. W. Vincent and D. D. Wright, Combustor Design Fundamentals, 14th Symposium (International) on Combustion, The Combustion Institute, Pittsburgh, Pa., 1973, pp. 627-638.

7. D. C. Lilley and D. L. Rhode, A Computer Code for Swirling Turbulent Axisymmetric Recirculating Flows in Practical Isothermal Combustor Geometries. NASA CR-3442, 1982.

8. L. Krishnamurthy, Numerical Modelling of Flowfield in a Dump Combustor. Fifth Annual Mini Symposium on Aerospace Science and Technology, AFIT, Wright-Patterson AFB, Ohio, 1979.

9. H. McDonald, Combustion Modelling in Two and Three Dimensions - Some Numerical Considerations, Prog, Energy Combust Sci, 1979, Vol. 5, pp 97-122.

10. B. E. Launder and D. B. Spalding, The Numerical Computation of Turbulent Flows, Computer Methods in Applied Mechanics and Engineering 3 (1974) 269-289.

11. A. D. Gosman and W. H. Pun, Calculation of Recirculating Flows. Report No. HTS/74/12, 1974, Dept. of Mechanical Engineering, Imperial College, London, England.

12. A. D. Gosman and F. J. K. Ideriah, TEACH-2E: A General Computer Program for Two-Dimensional, Turbulent, Recirculating Flows Report. Dept. of Mechanical Engineering, Imperial College, London, England, June 1976.

13. G. Winterfeldt, Private Communication, 1982.

REFERENCES (Continued)

14. S. K. Srivatsa, Computations of Soot and Emissions from Gas Turbine Combustors, NASA CR-167930, 1982.

15. J. E. Drewry, Characterization of Sudden-Expansion Dump Combustor Flowfields. AFAPL-TR-76-52, 1976.

16. P. L. Buckley, R. R. Craig, D. L. Davis and K. G. Schwartzkopf. The Design and Combustion Performance of Practical Swirlers for Integral Rocket/Ramjets. AIAA Paper No. 80-1119, Hartford, Connecticut, June 30 - July 2, 1982.

17. L. Krishnamurthy, Private Communication, 1982.

18. R. S. Boray and C. Chang, Flow Studies of Dump Combustors. Fifth International Symposium on Airbreathing Engines, February 16-21, 1981, Bangalore, India.

19. D. L. Rhode and D. G. Lilley, Mean Flowfields in Axisymmetric Combustor Geometries with Swirl. AIAA Paper 82-0177, Orlando, Florida, January 11-14, 1982.

20. S. A. Syed and A. J. Sturgess, Validation Studies of Turbulence and Combustion Models for Aircraft Gas Turbine Combustors. ASME Symposium: "Momentum and Heat Transfer Processes in Recirculating Flows," HTD-Vol 13, Chicago, 1980.

21. J. C. Putt, Fundamental Modelling of Three-Dimensional Two-Phase Reacting Flow Systems. January 1980 Annual Report, AFOSR Contract 78-0072.

22. M. E. Erdogan, F. Boyson and Swithenbank, J., Calculation of Reynolds Stresses. University of Sheffield, Dept. of Chemical Engineering and Fuel Technology, Report HIC 347, 1981.